A Finite-Element Surface-Water Model of Flow-Way Cell 1 of the Everglades Nutrient Removal Project, South Florida

Water-Resources Investigations Report 97-4159

Prepared in cooperation with the South Florida Water Management District

U.S. Department of the Interior
U.S. Geological Survey

A FINITE-ELEMENT SURFACE-WATER MODEL OF FLOW-WAY CELL 1 OF THE EVERGLADES NUTRIENT REMOVAL PROJECT, SOUTH FLORIDA

By Jonathan K. Lee and Mariano Guardo

U.S. GEOLOGICAL SURVEY

Water-Resources Investigations Report 97-4159

Prepared in cooperation with the

SOUTH FLORIDA WATER MANAGEMENT DISTRICT

Reston, Virginia

1998

U.S. DEPARTMENT OF THE INTERIOR
BRUCE BABBITT, Secretary

U.S. GEOLOGICAL SURVEY
Charles G. Groat, Director

For additional information
write to:

U.S. Geological Survey
Branch of Regional Research
Mail Stop 430
Reston, Virginia 20192

Copies of this report may be
purchased from:

U.S. Geological Survey
Branch of Information Services
Box 25286
Denver, Colorado 80225-0286

CONTENTS

FIGURES

FIGURES (Continued)

FIGURES (Continued)

TABLES

CONVERSION FACTORS AND VERTICAL DATUM

Multiply	By	To obtain
inch (in)	25.40	millimeter (mm)
inch per hour (in/h)	25.40	millimeter per hour (mm/h)
inch per day (in/d)	25.40	millimeter per day (mm/d)
foot (ft)	0.3048	meter (m)
foot per day (ft/d)	0.3048	meter per day (m/d)
foot per second (ft/s)	0.3048	meter per second (m/s)
mile (mi)	1.609	kilometer (km)
mile per hour (mi/h)	1.609	kilometer per hour (km/h)
square foot (ft^2)	0.09290	square meter (m^2)
square foot per second (ft^2/s)	0.09290	square meter per second (m^2/s)
acre	0.4047	hectare (ha)
cubic foot per second (ft^3/s)	0.02832	cubic meter per second (m^3/s)

National Geodetic Vertical Datum of 1929 (NGVD of 1929): A geodetic datum derived from a general adjustment of first-order level nets of both the United States and Canada, formerly called mean sea level, is referred to as sea level in this report.

A FINITE-ELEMENT SURFACE-WATER MODEL OF FLOW-WAY CELL 1 OF THE EVERGLADES NUTRIENT REMOVAL PROJECT, SOUTH FLORIDA

By Jonathan K. Lee and Mariano Guardo

Abstract

The Everglades Nutrient Removal (ENR) Project is a 3,815-acre wetland constructed by the South Florida Water Management District as a prototype to refine procedures for the design and operation of wetlands created for the biological removal of phosphorus and other contaminants from agricultural runoff before they enter the Everglades. The project was constructed in an area formerly used for agriculture, and a network of submerged irrigation and drainage canals and ditches exists within the project area. The canals may allow some water to move through the project too rapidly for optimal removal of contaminants. In an attempt to reduce flow in the canals in Flow-Way Cell 1, one of four treatment cells within the project, fill was placed at seven locations in each of two north-south canals in the cell.

The U.S. Geological Survey, in cooperation with the South Florida Water Management District, developed a two-dimensional, depth-averaged model for simulating surface-water flow in a wetland to help project engineers and managers understand the effects of submerged canals, flow resistance due to vegetation, wind, levee seepage, and ground-water inflows and outflows on flow velocities and water-surface elevations in the ENR Project and other constructed wetlands. The model was implemented and calibrated for Flow-Way Cell 1 of the ENR Project with data collected during the period March 17–21, 1996, when flow conditions in the cell were approximately steady and there was a persistent wind from the southwest. Roughness coefficients were determined during the calibration process. Several additional simulations were performed to determine effects of submerged canals, canal plugs, and wind on flow distribution and water-surface elevations.

The following results were obtained from the simulations:

- Manning's n values of 0.27 for cattail marsh with numerous small ditches and 0.18 for shallow open water with submersed vegetation and

sugar-cane stubble resulted in close agreement between observed and computed water-surface elevations and velocities.

- Water in marsh with either submersed or emergent vegetation flowed toward the south southwest, parallel to the levees on the east and west sides of Flow-Way Cell 1.
- Water flowed from north to south in north-south canals and from east to west in east-west canals.
- Canal plugs caused a large reduction in canal discharge at the plugs and a small reduction in canal discharge between plugs.
- Wind had an appreciable effect on flow distribution and water-surface slope in the southern half of Cell 1, where much of the marsh was open with submersed vegetation.

Introduction

The Everglades Nutrient Removal (ENR) Project is a 3,815-acre wetland constructed by the South Florida Water Management District (the District) as a prototype to refine procedures for the design and operation of wetlands created for the biological removal of phosphorus and other contaminants from agricultural runoff before they enter the Everglades. The project was constructed in an area formerly used for agriculture, and a network of submerged irrigation and drainage canals and ditches exists within the project area. The canals may allow some water to move through the project too rapidly for optimal removal of contaminants. In an attempt to reduce flow in the canals in Flow-Way Cell 1, one of four treatment cells within the project, fill was placed at seven locations in each of two north-south canals in the cell.

Because of interest by the the District in ensuring optimal performance of the ENR Project, the U.S. Geological Survey, in cooperation with the District, undertook a study to

- Develop a two-dimensional, depth-averaged model for simulating surface-water flow in a wetland to help project engineers and managers understand the effects of submerged canals, flow resistance due to vegetation, wind, levee seepage, and ground-water inflows and outflows on flow velocities and water-surface elevations in the ENR Project and other constructed wetlands;

- Implement and calibrate the model for approximately steady flow in Flow-Way Cell 1 of the ENR Project with data supplied by the District;

- Determine values for flow-resistance coefficients in Cell 1; and

- Determine effects of submerged canals, canal plugs, and wind on flow distribution and water-surface elevations in Cell 1.

Enhancements were made to the two-dimensional, depth-averaged finite-element surface-water model FESWMS-2DH (Froehlich, 1989; Lee and Froehlich, 1989) to make it suitable for modeling flow in wetlands. The enhanced model accounts for precipitation; evapotranspiration; ground-water inflow, or outflow, or both; sheltering of the water surface from wind by emergent vegetation; seepage through and under levee segments; and the effects on culvert flow, weir-segment flow, and levee-segment seepage of water-surface

elevations outside the wetland. The enhancements to the model are described in an addendum (Lee, 1998) to the original users manual (Froehlich, 1989).

The purposes of this report are to describe the implementation and calibration of the model for Flow-Way Cell 1 of the ENR Project and to present findings on flow resistance and effects of submerged canals, canal plugs, and wind on flow velocities and water-surface elevations in the cell.

The report first describes the ENR Project and the hydrology of the project area. Features of the model are then presented with emphasis on those most relevant to surface-water flow in wetlands. These features are flow resistance due to bed roughness and vegetative drag, wind, precipitation, evapotranspiration, ground-water inflows and outflows, and flow through culverts and through and under levees. The numerical solution of the equations is discussed. The report next describes the design of the finite-element grid for Cell 1 and discusses implementation of the model for data collected in Cell 1 during the period March 17–21, 1996. The discussion of model calibration includes subsections on calibration data, the calibration process, and comparison of observed and computed data. The report presents results of three additional simulations to examine the effects of submerged canals, canal plugs, and wind.

The units of dimensioned parameters and variables are given in the text in terms of length (L), time (T), and mass (M). All data used in the development of the model are available in the files of the South Florida Water Management District in West Palm Beach, Fla.

The Everglades Nutrient Removal Project

The ENR Project (fig. 1) is a 3,815-acre wetland constructed by the South Florida Water Management District as a prototype to refine procedures for the design and operation of wetlands created for the biological removal of phosphorus and other contaminants from agricultural runoff before they enter the Everglades. The project is located in south Florida, about 20 mi west of the city of West Palm Beach, and treats agricultural drainage from the Everglades Agricultural Area (EAA) to the north and west of the project before it enters the Loxahatchee National Wildlife Refuge, also known as Water Conservation Area 1 (WCA-1), to the south and east. In the 1930s, the site was drained and converted from natural Everglades marshes, wet prairies, sloughs, and swamps to agricultural uses. Since that time, about 5

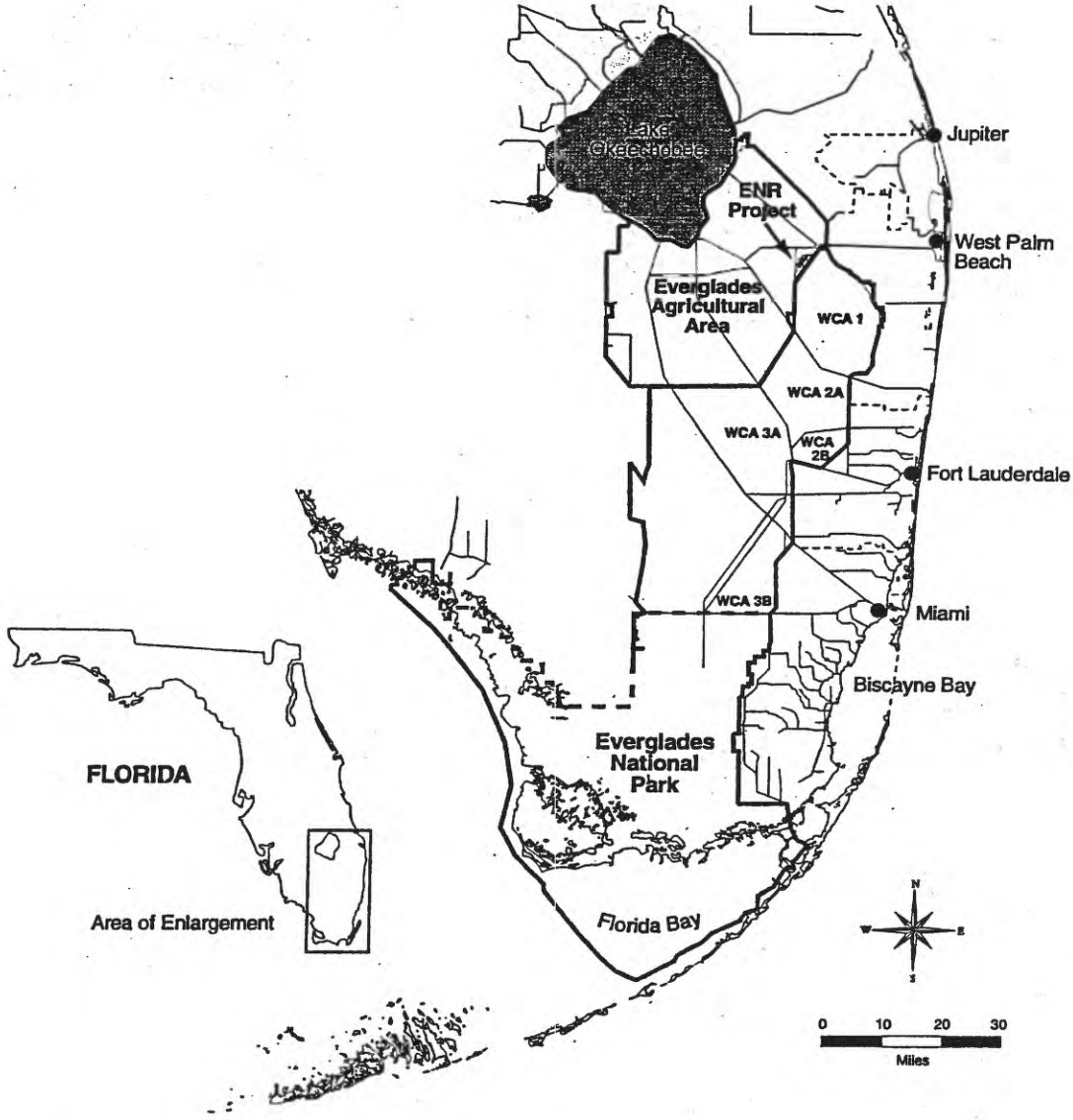

Figure 1: Location of the Everglades Nutrient Removal (ENR) Project in south Florida.

ft of the top peat soil has been lost because of oxidation and subsidence. At present, 3 to 7 ft of peat overlays limestone rock (Jammal and Associates, 1991). A network of submerged north-south and east-west ditches and canals within the ENR Project remains from years of agricultural use. The District has blocked each of the two largest north-south canals in Flow-Way Cell 1 with seven plugs, each of which consists of earthen fill approximately to the top of the canal banks.

The average ground-surface elevation of the project is 10 ft above sea level. Important features of the ENR Project are shown in figure 2. The project is surrounded by a levee and divided by interior levees into four treatment cells. The L-7 levee along the southeast side of the project forms part of the perimeter levee and separates the project from WCA-1. The northern two parallel cells (Cells 1 and 2), called flow-way cells, have been revegetated through natural growth of cattails. The southern two cells (Cells 3 and 4) are called polishing cells. Cell 3 has been planted with mixed marsh vegetation. Emergent vegetation has been controlled in Cell 4 to allow a submersed macrophyte/algal system to dominate. Cells 1 through 4 are 1,297, 1,023, 938, and 361 acres in size, respectively. Two groups of fifteen 0.5-acre test cells, one in the northeast corner of Cell 1 and the other in the northeast corner of Cell 3, are used for research on nutrient removal.

A 2.1-mile-long supply canal diverts part of the agricultural drainage from the EAA to the project. Six pumps with a total capacity of 600 ft^3/s move water from the supply canal into a 135-acre Buffer Cell for distribution to Cells 1 and 2 through a series of culverts. Each of the 10 culverts (G-252A through G-252J) conveying water into Cell 1 and each of the five culverts (G-255A through G-255E) (fig. 2) conveying water into Cell 2 is made of corrugated metal pipe, 6 ft in diameter, and is equipped with a riser, 7 ft in diameter (crest width), and stop logs for control of flows and water depths. Water moves from Cell 1 to Cell 3 and from Cell 2 to Cell 4. The two treatment streams are separated by an interior levee extending from northeast to southwest. Flow is conveyed from Cell 1 to Cell 3 through 10 structures (G-253A through G-253J) similar to those conveying water into Cell 1, except that the risers are 12 ft in diameter. Flow is conveyed from Cell 2 to Cell 4 through five structures (G-254A through G-254E). The invert elevation of all these culverts is 5 ft above sea level. Consequently, they usually flow fully submerged. Water from both treatment streams is conveyed by a collection canal to six pumps with a capacity of 450 ft^3/s for discharge into the L-7 borrow canal that forms the western boundary of

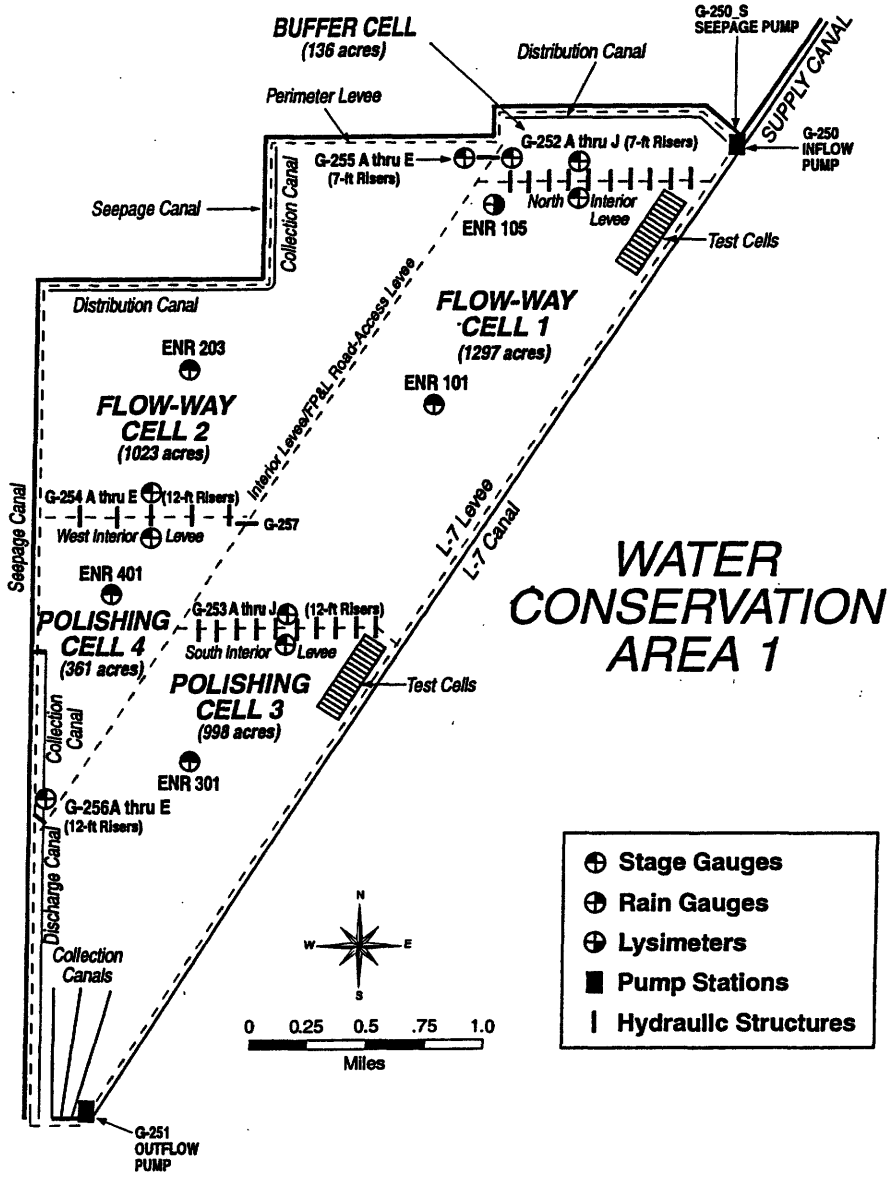

Figure 2: The Everglades Nutrient Removal Project in south Florida.

WCA-1. These features of the ENR Project are shown in figure 2.

Hydrology of the ENR Project

The capability of the ENR Project to remove contaminants from agricultural runoff depends on the length of time contaminated water entering the project area is in contact with vegetation and, consequently, on how water moves through the project. The movement of water through the project is affected by the ground-surface slope, the presence of former irrigation and drainage canals, flow resistance due to bed roughness and vegetative drag, inflows, ouflows, seepage of water into or out of the system through and under levees and through the bed, rainfall, evapotranspiration, and wind. The relative magnitude of these factors changes with the seasons. The District has developed a comprehensive monitoring and research program to quantify the major processes and evaluate their significance in determining water-surface elevations and flows throughout the project. As part of this effort, water budgets have been calculated from surface inflow and outflow, precipitation, evapotranspiration, and seepage data (Guardo, 1996).

To calculate storage of water within the ENR Project, an extensive stage-monitoring system was established. Water levels are recorded continuously at gages within the project. Stations at which stages are recorded within Cell 1 are shown in figure 3. These include three stations (G-252AB, G-252EF, and G-252IJ) near the culverts through which water flows into the cell, three stations (G-253AB, G-253EF, and G-253IJ) near the culverts through which water flows out of the cell, and one station (ENR101) near the center of the cell.

Pump-operation records provide data on discharges into the Buffer Cell from the supply canal and into the L-7 borrow canal from the outflow collection canal. From historical data, velocities less than 0.2 ft/s result 30 percent of the time in the culverts connecting the cells of the project. Ultrasonic velocity meters, which are accurate at low velocities and have low susceptibility to fouling, were installed in the culverts to determine surface inflow to and outflow from each cell (Guardo and others, 1994; Guardo and others, 1995). Ultrasonic velocity meters were installed in the 10 culverts (G-252A through G-252J) conveying water to Cell 1 and in the 10 culverts (G-253A through G-253J) conveying water from Cell 1 to Cell 3. For the time period March 17–21, 1996, used for model calibration, the average flow

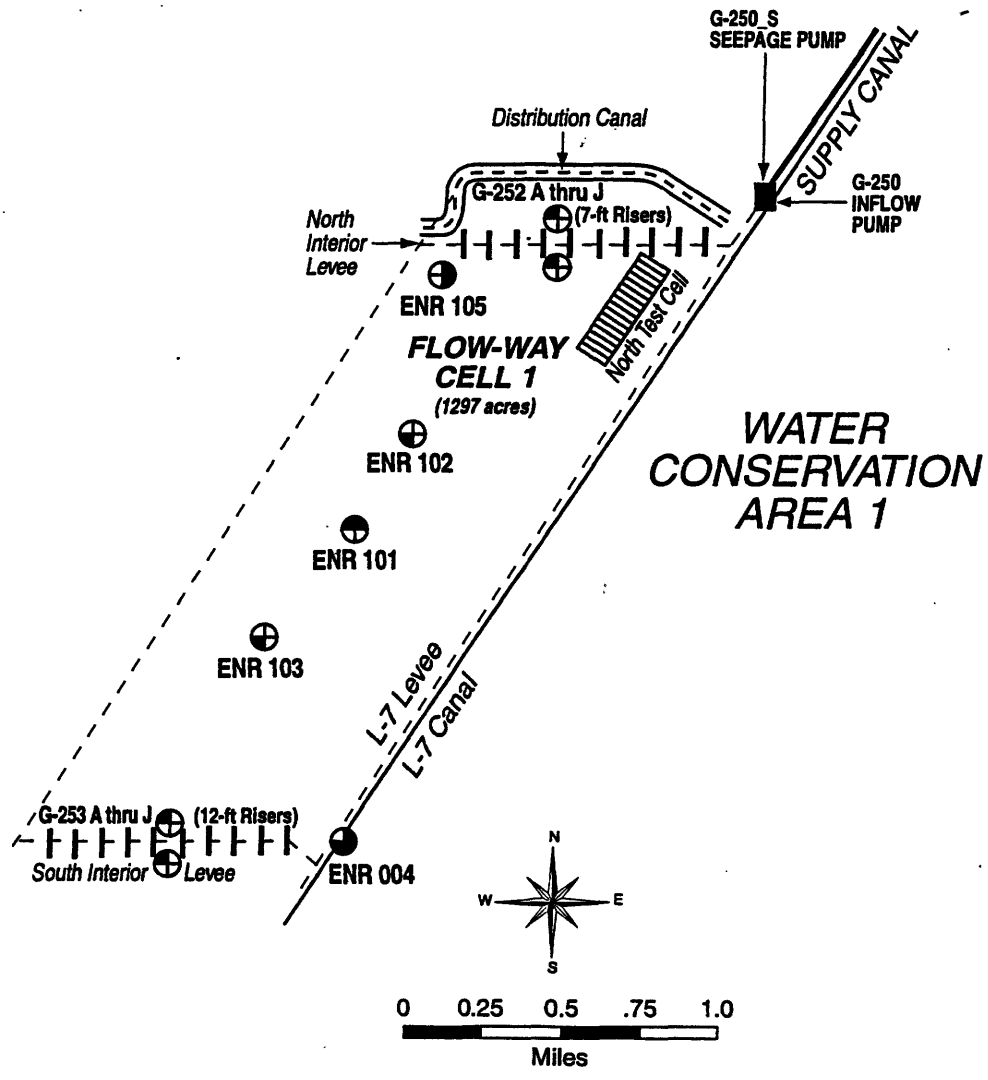

Figure 3: Cell 1 of the Everglades Nutrient Removal Project in south Florida showing structures and instrumentation sites.

velocity in the culverts was about 1.2 ft/s.

From records from 1929 to 1991, the average annual rainfall for the EAA, where the ENR Project is located, is 52.4 in (Abtew and Khanal, 1994). On average, 66 percent of the annual rain falls during the wet season from early June to late October. A network of 10 continuously recording, tipping-bucket rain gages was established to accurately measure rainfall within the project and assess the spatial and temporal variability of rainfall. After further analysis of the rainfall within the ENR Project, the rain-gage network was reduced to seven sites after September 1995 (Guardo, 1996). For this study, which involved only Cell 1, rainfall data were taken from station ENR101, which is located at the center of the cell (fig. 3).

Three lysimeters were installed to measure evapotranspiration in cattails, mixed vegetation, and open water. Concurrent weather data are collected at each lysimeter site for use in calibration of the Penman-Monteith equation for the site (Abtew, 1996). The locations of the lysimeters are shown in figure 2. On the basis of vegetation maps obtained from infrared aerial photographs, which are taken approximately twice every year by the District, the vegetation coverage is estimated for each of the three vegetation types (Guardo, 1996). Daily-average evapotranspiration values are obtained from the lysimeter data and the vegetation-coverage information.

Wind magnitude and direction are collected at station ENR105, which is located in the northwest corner of Cell 1 (fig. 3). Wind magnitude is recorded in miles per hour, and the direction from which the wind is blowing is recorded in degrees clockwise from north.

To estimate levee seepage into and out of the ENR Project and between cells, 15 piezometers and 11 pairs of staff gages were installed along the perimeter and interior levees. Staff gages and piezometers are read concurrently to measure head gradients across the levees. Guardo (1996) obtained an equation for surficial seepage emerging into Cells 1 and 3 through the L-7 levee from regression of instantaneous flows measured approximately every 2 weeks from August 1994 through June 1996 on mean daily water-surface elevations in WCA-1 and Cells 1 and 3. Prymas (1997) developed a regression equation for subsurface seepage under the L-7 levee by using results from a calibrated finite-element levee-seepage model and the same flow and water-surface-elevation data used to develop the equation for surficial seepage.

A Model for Surface-Water Flow in Wetlands

The two-dimensional, depth-averaged finite-element model FESWMS-2DH (Froehlich, 1989; Lee and Froehlich, 1989) was enhanced for use in wetland environments (Lee, 1998) and used to simulate flows in Cell 1 of the ENR Project. The finite-element approach is ideally suited to simulating shallow, two-dimensional flow over complex topography having spatially variable resistance to flow. A two-dimensional finite-element surface-water model with depth and depth-averaged velocity components as dependent variables allows the user great flexibility in defining geometric features such as water-body boundaries, channels, and levees. The model user is able to use a fine grid in regions where geometric or flow gradients are large and a coarse grid in regions where geometry and flow are more nearly uniform. In addition, the introduction of complex boundary conditions is easily handled in the finite-element approach.

The enhanced flow model is capable of simulating steady or unsteady two-dimensional flow in the horizontal plane. The vertically integrated equations of motion and continuity are solved for depth and depth-averaged velocity components at the node points of the finite-element grid. Flow resistance, turbulent stresses, and wind stresses are simulated in the model. Precipitation, evapotranspiration, and ground-water inflows and outflows can be simulated. Flow over weirs, through culverts, and through and under levees also can be modeled.

Depth-Averaged Flow Equations

The depth-averaged flow equations for conservation of momentum in the x- and y-directions and conservation of mass are given in Froehlich (1989, p. 1-4-2). The momentum equations are

$$\frac{\partial(HU)}{\partial t} + \frac{\partial(\beta_{uu}HUU)}{\partial x} + \frac{\partial(\beta_{uv}HUV)}{\partial y} + gH\frac{\partial z_b}{\partial x} + \frac{g}{2}\frac{\partial H^2}{\partial x} - \Omega HV + \frac{1}{\rho}\left[\tau_x^b - \tau_x^s - \frac{\partial(H\tau_{xx})}{\partial x} - \frac{\partial(H\tau_{xy})}{\partial y}\right] = 0 \qquad (1)$$

in the x-direction and

$$\frac{\partial(HV)}{\partial t} + \frac{\partial(\beta_{vu}HVU)}{\partial x} + \frac{\partial(\beta_{vv}HVV)}{\partial y} + gH\frac{\partial z_b}{\partial y} + \frac{g}{2}\frac{\partial H^2}{\partial y} + \Omega HU + \frac{1}{\rho}\left[\tau_y^b - \tau_y^s - \frac{\partial(H\tau_{yx})}{\partial x} - \frac{\partial(H\tau_{yy})}{\partial y}\right] = 0 \quad (2)$$

in the y-direction, and the continuity (conservation-of-mass) equation is

$$\frac{\partial H}{\partial t} + \frac{\partial(HU)}{\partial x} + \frac{\partial(HV)}{\partial y} - q = 0, \quad (3)$$

where x, y = Cartesian coordinates in the positive east and north directions, respectively (L); t = time (T); U, V = depth-averaged velocity components in the x- and y-directions, respectively (L/T); H = depth of flow (L); $\beta_{uu}, \beta_{uv}, \beta_{vu}, \beta_{vv}$ = momentum-correction coefficients that account for the variation of velocity in the vertical direction (dimensionless); z_b = bed elevation (L); ρ = density of water (assumed constant) (M/L^3); $\Omega = 2\omega \sin\phi$ = Coriolis parameter (1/T); ω = magnitude of the angular velocity of the Earth (1/T); ϕ = latitude; g = gravitational acceleration (L/T^2); $\tau_{xx}, \tau_{xy}, \tau_{yx}, \tau_{yy}$ = components of the depth-averaged effective-stress tensor (M/L/T^2); τ_x^s, τ_y^s = components of the surface stress (wind) in the x- and y-directions, respectively (M/L/T^2); τ_x^b, τ_y^b = components of the bottom stress and vegetative drag (friction) in the x- and y-directions, respectively (M/L/T^2); and q = source/sink term (L/T).

Equations 1 through 3 are commonly referred to as the shallow-water equations. These equations are obtained from the three-dimensional Reynolds equations for turbulent flow by integrating with respect to the water depth under the assumption of hydrostatic pressure and by making simplifying assumptions regarding the nonlinear terms. Lynch (1986) may be consulted for more information.

The first three terms of equations 1 and 2 are inertial-force terms. The first of the three represents temporal acceleration and the second and third represent convective acceleration. The momentum-correction coefficients result from the vertical integration of the equations of motion and account for the fact that when the vertical velocity profile is not uniform, the integral of the product of two velocity profiles is not equal to the product of the integrals. The fourth and fifth terms represent the pressure force due to the water-surface gradient. The sixth term represents the Coriolis force, an inertial force accounting for the effect of the Earth's rotation. The seventh term

in equations 1 and 2 represents the combination of bottom stress and vegetative drag, and the eighth term represents surface stress. The ninth and tenth terms represent the combined effects of viscous stresses and Reynolds stresses. Additional information on momentum-correction coefficients, the Coriolis parameter, and bed, surface, and turbulent stresses can be found in the original users manual (Froehlich, 1989, p. 1-4-5—1-4-11) and the addendum to the users manual (Lee, 1998).

Flow Resistance due to Bed Roughness and Vegetative Drag

The directional components, τ_x^b and τ_y^b, of flow resistance due to bed roughness and vegetative drag are

$$\tau_x^b = \rho c_f U (U^2 + V^2)^{1/2} \left[1 + \left(\frac{\partial z_b}{\partial x} \right)^2 + \left(\frac{\partial z_b}{\partial y} \right)^2 \right]^{1/2} \tag{4}$$

and

$$\tau_y^b = \rho c_f V (U^2 + V^2)^{1/2} \left[1 + \left(\frac{\partial z_b}{\partial x} \right)^2 + \left(\frac{\partial z_b}{\partial y} \right)^2 \right]^{1/2}, \tag{5}$$

where c_f = flow-resistance coefficient (dimensionless). The coefficient c_f is computed as

$$c_f = \frac{g n^2}{\phi H^{1/3}}, \tag{6}$$

where n = Manning's roughness coefficient and $\phi = 2.208$ when inch/pound units are used and 1.0 when SI units are used. Manning's roughness coefficients are allowed to vary with space, time, and depth in the model.

Surface Shear Stress

The directional components, τ_x^s and τ_y^s, of the surface shear stress are

$$\tau_x^s = c_s \rho_a W^2 \cos\psi \tag{7}$$

and

$$\tau_y^s = c_s \rho_a W^2 \sin\psi, \tag{8}$$

where c_s = surface-stress coefficient (dimensionless); ρ_a = density of air (M/L^3); W = characteristic wind velocity near the water surface (L/T);

and ψ = angle measured counterclockwise from the positive x-axis to the direction toward which the wind is blowing. Additional information on evaluating c_s can be found in Froehlich (1989, p. 1-4-8). Wind is allowed to vary in both space and time.

To account for the sheltering effect of emergent vegetation, τ_x^s and τ_y^s are multiplied by a dimensionless sheltering coefficient, S, defined by Reid and Whitaker (1976, p. 64) for $h_v > H$ as

$$S = \frac{1}{1 + \dfrac{c_v N_v w_v (h_v - H)}{c_s}}, \tag{9}$$

where c_v = vegetation drag coefficient (dimensionless), N_v = plant density, in stems or leaves per unit area ($1/L^2$), w_v = average stem or leaf width (L), and h_v = average stem or leaf height (L). The parameters c_v, N_v, w_v, and h_v are allowed to vary in both space and time. Assigning a value to c_v is discussed in Reid and Whitaker (1976, p. 68). For $h_v \leq H$, S is assigned the value 1.0.

Turbulent Stresses

By Boussinesq's eddy-viscosity concept, the depth-averaged turbulent stresses are written

$$\tau_{xx} = \rho \hat{\nu}_{xx} \left(\frac{\partial U}{\partial x} + \frac{\partial U}{\partial x} \right), \tag{10}$$

$$\tau_{xy} = \tau_{yx} = \rho \hat{\nu}_{xy} \left(\frac{\partial U}{\partial y} + \frac{\partial V}{\partial x} \right), \tag{11}$$

and

$$\tau_{yy} = \rho \hat{\nu}_{yy} \left(\frac{\partial V}{\partial y} + \frac{\partial V}{\partial y} \right), \tag{12}$$

where $\hat{\nu}_{xx}, \hat{\nu}_{xy}, \hat{\nu}_{yx}, \hat{\nu}_{yy}$ = depth-averaged kinematic eddy viscosities (turbulent exchange coefficients) (L^2/T). In the model, it is assumed that the depth-averaged kinematic eddy viscosity is isotropic and is denoted by $\hat{\nu}$; that is,

$$\hat{\nu} = \hat{\nu}_{xx} = \hat{\nu}_{xy} = \hat{\nu}_{yx} = \hat{\nu}_{yy}. \tag{13}$$

In natural open channels, the eddy viscosity has been shown to be related to the bed shear velocity and the depth by

$$\hat{\nu} = (0.6 \pm 0.3) U_* H, \tag{14}$$

where $U_* = c_f^{1/2}(U^2 + V^2)^{1/2}$ = bed shear velocity (L/T) (Froehlich, 1989, p. 1-4-10). Here the eddy viscosity is represented as

$$\hat{\nu} = \hat{\nu}_0 + c_\mu U_* H, \tag{15}$$

where $\hat{\nu}_0$ = base kinematic eddy viscosity (L^2/T) and c_μ = dimensionless coefficient. In some cases, a small positive value of $\hat{\nu}_0$ is required for numerical stability of the finite-element solution.

Source/Sink Terms

The source/sink term, q, in equation 3 can be expanded to represent precipitation, evapotranspiration, and ground-water inflow, or outflow, or both. Thus,

$$q = q_p - q_e + q_g, \tag{16}$$

where q_p = precipitation rate (L/T); q_e = evapotranspiration rate (L/T); and q_g = ground-water-inflow or -outflow rate (L/T), positive for inflow and negative for outflow. These rates are permitted to vary in both space and time.

Ground-Water Inflow/Outflow

Seepage between surface water and ground water, q_g, is expressed as in McDonald and Harbaugh (1988, chap. 6). The surface water is assumed to be separated from the ground water by a low-permeability layer of material of thickness M_ℓ (L) (fig. 4). The hydraulic conductivity of this layer is denoted by K_ℓ (L/T). If it is further assumed that all head losses between the surface water and the aquifer are across the low-permeability layer and that the piezometric head of the ground water is above the bottom of the low-permeability layer, then the flow, q_g, between the surface water and the aquifer is given by

$$q_g = \frac{K_\ell}{M_\ell}(z_g - z_b - H) = C_\ell(z_g - z_b - H), \tag{17}$$

where $C_\ell = K_\ell/M_\ell$ = hydraulic conductance of the low-permeability layer (1/T) and z_g = ground-water head (L). Note that q_g is positive (the flow is from the ground water to the surface water) if $z_g > z_b + H$ and q_g is negative if $z_g < z_b + H$. As discussed in McDonald and Harbaugh (1988, chap. 6), if the ground-water level falls below a certain point, flow from the surface

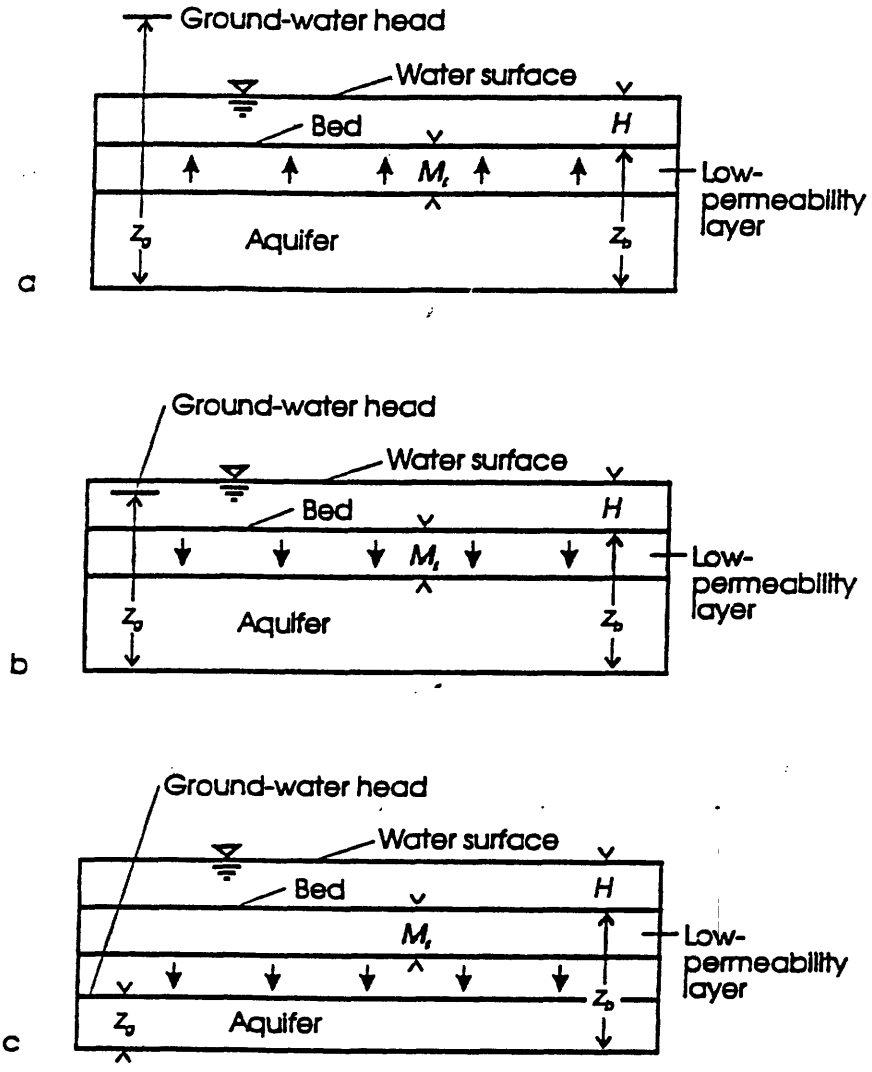

Figure 4: Conceptual representation of surface-water/ground-water interconnection with (a) the ground-water head above the surface-water elevation, (b) the ground-water head below the surface-water elevation but above the bottom of the low-permeability layer, and (c) the ground-water head below the bottom of the low-permeability layer.

water to the ground water no longer depends on the ground-water head. If the water level in the aquifer falls below the base of the low-permeability layer and if it is assumed that the low-permeability layer remains saturated, then the head at its base is the elevation of that point. Because the elevation of the base of the low-permeability layer is $z_b - M_\ell$, the flow, q_g, from the surface water to the ground water is

$$q_g = C_\ell(z_b - M_\ell - z_b - H) = -C_\ell(M_\ell + H). \tag{18}$$

Equations 17 and 18 can be combined to give

$$q_g = \begin{cases} C_\ell(z_g - z_b - H) & \text{if } z_g > z_b - M_\ell, \\ -C_\ell(M_\ell + H) & \text{if } z_g \leq z_b - M_\ell. \end{cases} \tag{19}$$

Finite-Element Grids and Interpolation

In the finite-element method, the physical domain of interest is divided into a finite number of subdomains called elements. An element may be either a triangle or a quadrilateral and is defined by a finite number of node points situated along its boundary or in its interior. Values of the dependent variables are uniquely defined within each element in terms of their values at the node points of the element by a set of interpolation functions.

The model FESWMS-2DH allows the use of six-node triangles and nine-node "Lagrangian" quadrilaterals (Pinder and Gray, 1977) for representing velocity components. Linear triangles or bilinear quadrilaterals are used to represent depth. In this study, only triangles were used. For each triangle, the three depth nodes are located at the vertices of the triangle, and the six velocity nodes are located at the vertices and the midsides of the three sides. Model topography is defined by assigning a ground-surface elevation to each element vertex and requiring the ground surface to vary linearly within each element.

Initial and Boundary Conditions

Both initial and boundary conditions must be specified to solve the system of depth-averaged flow equations. For initial conditions, flow depth and both velocity components must be specified throughout the flow domain. Boundary conditions must be specified for the entire boundary of the flow domain.

Velocities, unit discharges, flow depths, and relations between discharge and water-surface elevations can be specified.

Boundary segments may be either closed or open. Examples of closed boundaries are shorelines and levees. No net flow is permitted to cross a closed boundary unless a weir, culvert, or levee segment is present. At a closed boundary, a slip condition is said to be specified if flow is allowed to move tangent to the boundary. A no-slip condition is said to be specified if both normal and tangential components of velocity are set to zero. Slip conditions usually are applied. Flow may cross closed boundaries over weirs, through culverts, or as seepage through and under levees. In these cases, special stage-discharge relations are used to define discharge as a function of water-surface elevations at one or both ends of the structure.

Open boundaries include both inflow and outflow boundaries. For subcritical flow, either water-surface elevation or both components of unit discharge or velocity must be specified at an open boundary. For most subcritical-flow channel models, components of unit discharge are specified for inflow, and water-surface elevation is specified for outflow. The FESWMS-2DH users manual (Froehlich, 1989, p. 1-4-25—1-4-28) can be consulted for more information.

Flow through Culverts

One-dimensional flow through a fully submerged culvert is a function of the water-surface elevations at the two ends of the culvert and the physical characteristics of the culvert. Each culvert is described by either one or two boundary nodes and the cross-sectional area, hydraulic radius, length, and interior roughness of the culvert. Two boundary nodes are needed, one at each end of the culvert, if both ends of the culvert are included in the finite-element grid. Water that flows through a culvert defined by two boundary nodes (fig. 5) leaves the grid at the upstream node (the node with the higher water-surface elevation) and enters the grid at the downstream node. If only one end of a culvert is included in the grid, only one boundary node is needed for the culvert. In this case, the water-surface elevation outside the grid must be specified, and flow into or out of the grid is determined on the basis of the interior and specified exterior water-surface elevations. Bodhaine (1968) expresses flow, Q_c (L^3/T), through a fully submerged culvert as

$$Q_c = K_c(z_s^h - z_s^t)^{1/2}, \tag{20}$$

where z_s^h = water-surface elevation at the upstream end of the culvert (head-water elevation) (L); z_s^t = water-surface elevation at the downstream end of the culvert (tail-water elevation) (L); and K_c = culvert coefficient ($L^{5/2}/T$) and is defined as

$$K_c = C_c A_c \sqrt{2g} \left(1 + \frac{29 C_c^2 n_c^2 L_c}{\phi_c R_c^{4/3}}\right)^{-1/2}, \tag{21}$$

where C_c = discharge coefficient (dimensionless); A_c = cross-sectional area of the culvert (L^2); n_c = Manning's roughness coefficient of the culvert barrel; L_c = length of the culvert barrel (L); ϕ_c = 1.0 when inch/pound units are used and 1.486 when SI units are used; and R_c = hydraulic radius of the culvert barrel (L). For information on evaluating C_c, Froehlich (1989, p. 1-4-12—1-4-23) can be consulted.

Flow Through and Under Levees

One-dimensional seepage flow through and under a levee is modeled by dividing the levee into sections called levee segments. Each levee segment is described by either one or two boundary nodes and the base width, top width, height, and length of the levee segment. If water is allowed to flow under the levee, the thickness of the levee-segment sublayer must be given. Additionally, the permeabilities of the levee segment and the sublayer are required. Two boundary nodes are needed, one on each side of the segment, if both sides of the levee segment are included in the finite-element grid. Water that flows through or under a levee segment defined by two boundary nodes (fig. 5) leaves the grid at the upstream node (the node with the higher water-surface elevation) and enters the grid at the downstream node. If only one side of a levee segment is included in the grid, only one boundary node is needed for each levee segment. In this case, the water-surface elevation outside the grid must be specified, and flow into or out of the grid is determined on the basis of the interior and specified exterior water-surface elevations. Levee segments, weir segments, and culverts may share the same nodes, as shown in figure 5.

A definition sketch of the cross section of a permeable levee with a permeable sublayer is shown in figure 6. The angle, β, between the horizontal and the side of the levee is assumed to be the same for both sides. Then

$$\tan\beta = \frac{2h_\ell}{b_2 - b_1} \tag{22}$$

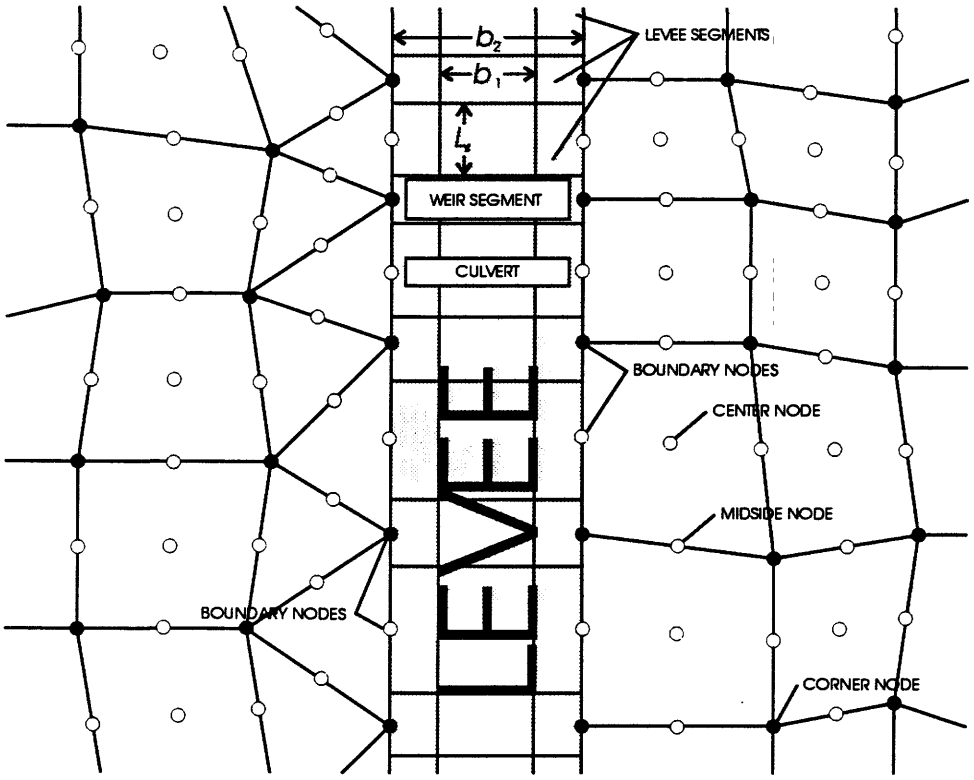

Figure 5: Finite-element grid with levee segments, a weir segment, and a culvert.

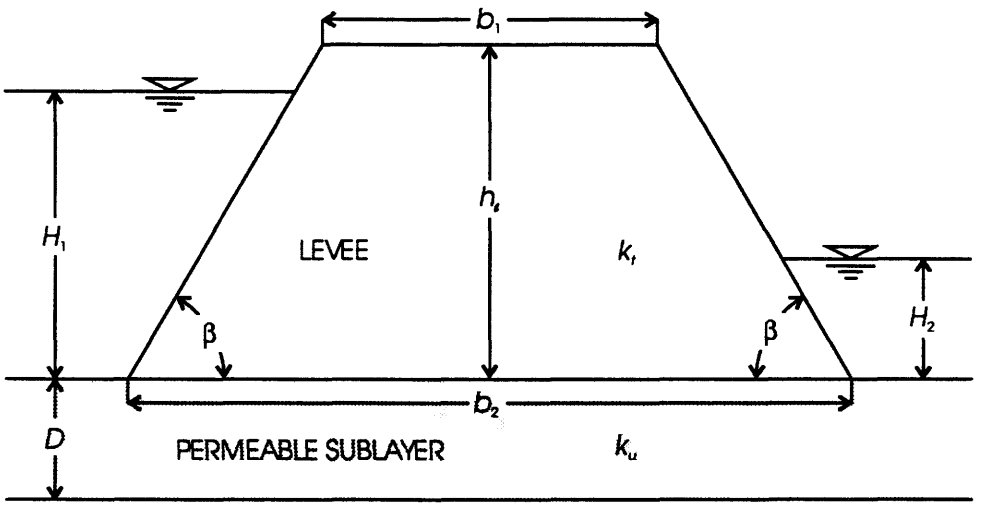

EXPLANATION

b_1	TOP WIDTH OF LEVEE	D	THICKNESS OF PERMEABLE SUBLAYER
b_2	BASE WIDTH OF LEVEE	H_1	FLOW DEPTH UPSTREAM FROM LEVEE
h_e	HEIGHT OF LEVEE	H_2	FLOW DEPTH DOWNSTREAM FROM LEVEE
k_f	PERMEABILITY OF LEVEE	β	ANGLE BETWEEN HORIZONTAL AND SIDE OF LEVEE
k_u	PERMEABILITY OF SUBLAYER		

Figure 6: Levee cross section.

or

$$\beta = \arctan\left(\frac{2h_\ell}{b_2 - b_1}\right), \tag{23}$$

where h_ℓ = height of the levee (L), b_2 = base width of the levee (L), and b_1 = top width of the levee (L). The symbol D denotes the thickness of the permeable sublayer (L), and k_t and k_u denote the permeabilities of the levee and the sublayer, respectively (L/T).

Peter (1982, p. 123) presents the following equation for the total seepage flow, q_ℓ, per unit length of levee segment (L^2/T):

$$q_\ell = q_t + q_u, \tag{24}$$

where

$$q_t = k_t \frac{H_1^2 - H_{2s}^2}{2d} \tag{25}$$

and (Department of the Army, 1978, p. B-13)

$$q_u = k_u \frac{(H_1 - H_2)D}{b_2\left(1 + 0.86\frac{D}{b_2}\right)}. \tag{26}$$

Here, q_t and q_u = seepage flow per unit length through and under the levee segment, respectively (L^2/T)); H_1 = depth of water on the upstream side of the levee segment (L); H_2 = depth of water on the downstream side of the levee segment (L); and

$$H_{2s} = H_s + H_2, \tag{27}$$

where H_s = height above the downstream water surface at which the seepage surface emerges on the downstream face of the levee (L) (fig. 7). It can be shown (Peter, 1982, p. 107) that the lower part of the seepage surface can be approximated by a parabola. The variable d in equation 25 is the length (L) of the projection on the horizontal of the line connecting the focus of the parabola and the point where the tangent of inflection to the parabola intersects the water surface (fig. 7). Thus, d can be approximated as

$$d = 0.3s_1 + s_2 + b_1 + s_3 - s_4. \tag{28}$$

The terms of equation 28 can be written

$$s_1 = H_1 \cot\beta, \tag{29}$$

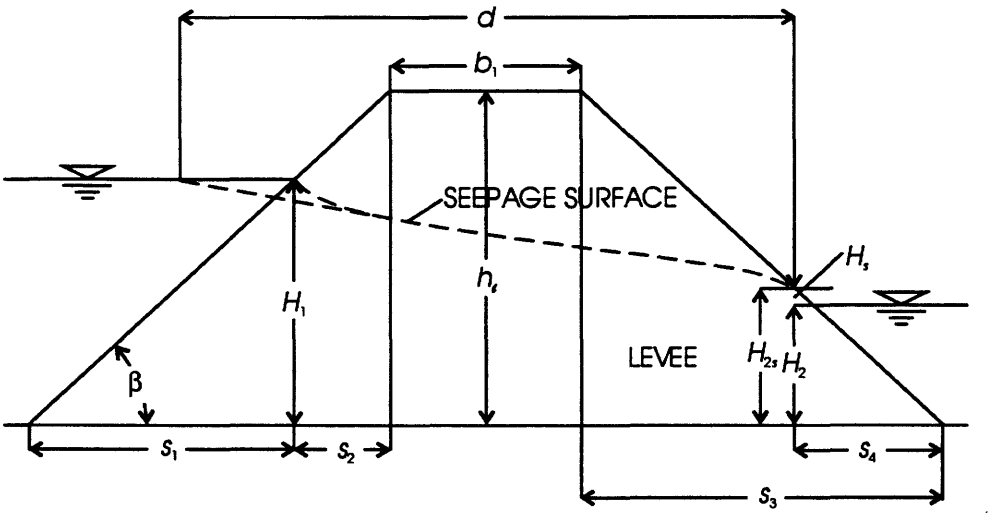

EXPLANATION

b_1	TOP WIDTH OF LEVEE	S_4	VARIABLE DEFINED IN EQUATION 4.20
d	VARIABLE DEFINED IN EQUATION 4.16	H_1	FLOW DEPTH UPSTREAM FROM LEVEE
h_t	HEIGHT OF LEVEE	H_2	FLOW DEPTH DOWNSTREAM FROM LEVEE
S_1	VARIABLE DEFINED IN EQUATION 4.17	H_{2s}	VARIABLE DEFINED IN EQUATION 4.15
S_2	VARIABLE DEFINED IN EQUATION 4.18	H_s	VARIABLE DEFINED IN EQUATION 4.21
S_3	VARIABLE DEFINED IN EQUATION 4.19	β	ANGLE BETWEEN HORIZONTAL AND SIDE OF LEVEE

Figure 7: Definition of levee-seepage parameters.

$$s_2 = (h_\ell - H_1)\cot\beta, \tag{30}$$

$$s_3 = h_\ell \cot\beta, \tag{31}$$

and

$$s_4 = (H_2 + H_s)\cot\beta = H_{2s}\cot\beta, \tag{32}$$

where

$$H_s = f(\beta)\frac{(H_1 - H_2)^2}{b_1 + b_2}, \tag{33}$$

and the function f is given in Peter (1982, p. 111) and the addendum to the users manual (Lee, 1998, p. 12). Substituting equations 29 through 33 into equation 28 gives

$$d = b_1 + \cot\beta\left[2h_\ell - 0.7H_1 - H_2 - f(\beta)\frac{(H_1 - H_2)^2}{b_1 + b_2}\right]. \tag{34}$$

By equations 25, 27, 33, and 34,

$$q_t = k_t \frac{H_1^2 - \left[H_2 + f(\beta)\dfrac{(H_1 - H_2)^2}{b_1 + b_2}\right]^2}{2\left\{b_1 + \cot\beta\left[2h_\ell - 0.7H_1 - H_2 - f(\beta)\dfrac{(H_1 - H_2)^2}{b_1 + b_2}\right]\right\}}. \tag{35}$$

Numerical Solution of the Flow Equations

The enhanced flow model uses the Galerkin finite-element method to solve the system of partial-differential equations and associated boundary conditions governing two-dimensional, depth-averaged, surface-water flow. The time derivatives are represented by an implicit finite-difference scheme. In this study, however, only the steady-state forms of the equations are solved.

The method of weighted residuals is applied to the governing differential equations to form a set of finite-element equations for each element. Approximations of the dependent variables in terms of interpolation functions and nodal unknowns are substituted into the governing equations to form residuals. The residuals are required to vanish in a weighted-average sense over the entire solution domain. In Galerkin's method, the weighting functions are chosen to be the same as those used to interpolate values of the dependent variables within each element. By requiring the weighted residuals to vanish

over the entire solution domain, the finite-element equations take on an integral form. Coefficients are integrated numerically, and all the element, or local, contributions are assembled to obtain the complete, or global, set of equations. Equations for nodal unknowns at which boundary conditions are specified are replaced by constraint equations representing the appropriate boundary conditions. The resulting set of nonlinear algebraic equations is solved simultaneously for the nodal values of the dependent variables. The global set of nonlinear algebraic equations is solved by the Newton-Raphson iteration method and a frontal solution algorithm using out-of-core storage. Additional information on the finite-element method can be found in Pinder and Gray (1977) and Zienkiewicz (1977). Details of the implementation of the finite-element method used in the enhanced version of FESWMS-2DH are described in Froehlich (1989), Lee and Froehlich (1989), and Lee (1998).

A Finite-Element Grid for Cell 1

Data made available by the District and the grid-generation software TRIGRID (Walters and Henry, 1997) were used to develop a finite-element grid representing the boundary, topography, and vegetative cover of Flow-Way Cell 1 of the ENR Project. Data sets available for use in defining the boundaries of Cell 1, locating and sizing the major canals, and determining marsh ground-surface elevations included

- Coordinates of points located on the project border (DS-1);
- Coordinates of points located on canal centerlines (DS-2);
- Coordinates and elevations of points located in or near canals (DS-3);
- Coordinates and elevations of points located in and near Cell 1 and on lines of constant elevation with 0.2-foot spacing (DS-4); and
- Coordinates and elevations of points in and near Cell 1 and located on a series of transects (DS-5).

All coordinates in these data sets are based on the Florida State Plane Coordinate System.

Boundaries of Cell 1 and the Canal-Berm System

Data sets DS-1 and DS-5 were used to locate the edge of water within Cell 1. Model boundaries were established on the basis of this information. The boundary adjoining the L-7 levee was moved about 500 ft to the northwest to exclude from the grid 11 short roadway embankments which extend from the levee road to a high-voltage power line parallel to the levee. Representing these features would have required many elements; eliminating them helped reduce computational time. The 15 test cells in the northeast corner of Cell 1 also were excluded from the grid because, under most conditions, little water flows into or out of them. For these reasons, the Cell 1 model area is 1,116 acres, 181 acres less than the area of the actual cell. The model boundary, points from DS-5 located at the edge of water, and canal intersections with the boundary are shown in figure 8. From information on canal centerlines in DS-2 and information on canal-bottom elevations in DS-3, the major canals were positioned within the boundaries of the model. All canals were represented by 50-foot-wide, triangular cross sections. A strip 38 ft wide was located next to each canal bank within the interior of Cell 1. These strips were used to facilitate representation of low berms that lay parallel to several of the canals. The boundaries of the canal-berm system and canal-bottom elevations are shown in figure 9.

The Ground-Surface-Interpolation Grid

A grid was created from which natural ground-surface elevations could be interpolated at node points of the model grid for Cell 1. Subsets of data sets DS-3 (points in or near canals) and DS-4 (points on lines of constant elevation with 0.2-foot spacing) were used in this process. Points in both data sets that lay near or outside the model boundary of Cell 1 were removed. Points remaining in DS-3 and not marked as natural ground-surface points were removed. Thus, all points located in canals or on spoil banks near canals were removed. The remaining points of DS-3 and DS-4 are shown in figures 10 and 11, respectively. In the last stage of the selection process, points less than 50 ft apart were removed from consideration unless the ground-surface elevations at the points differed by 0.2 ft or more. Finally, points were added to define the boundary of Cell 1, and points were added at the intersections of canals with the boundary (fig. 8). Intermediate points were interpolated along straight-line segments of the Cell 1 boundary. Elevations were assigned

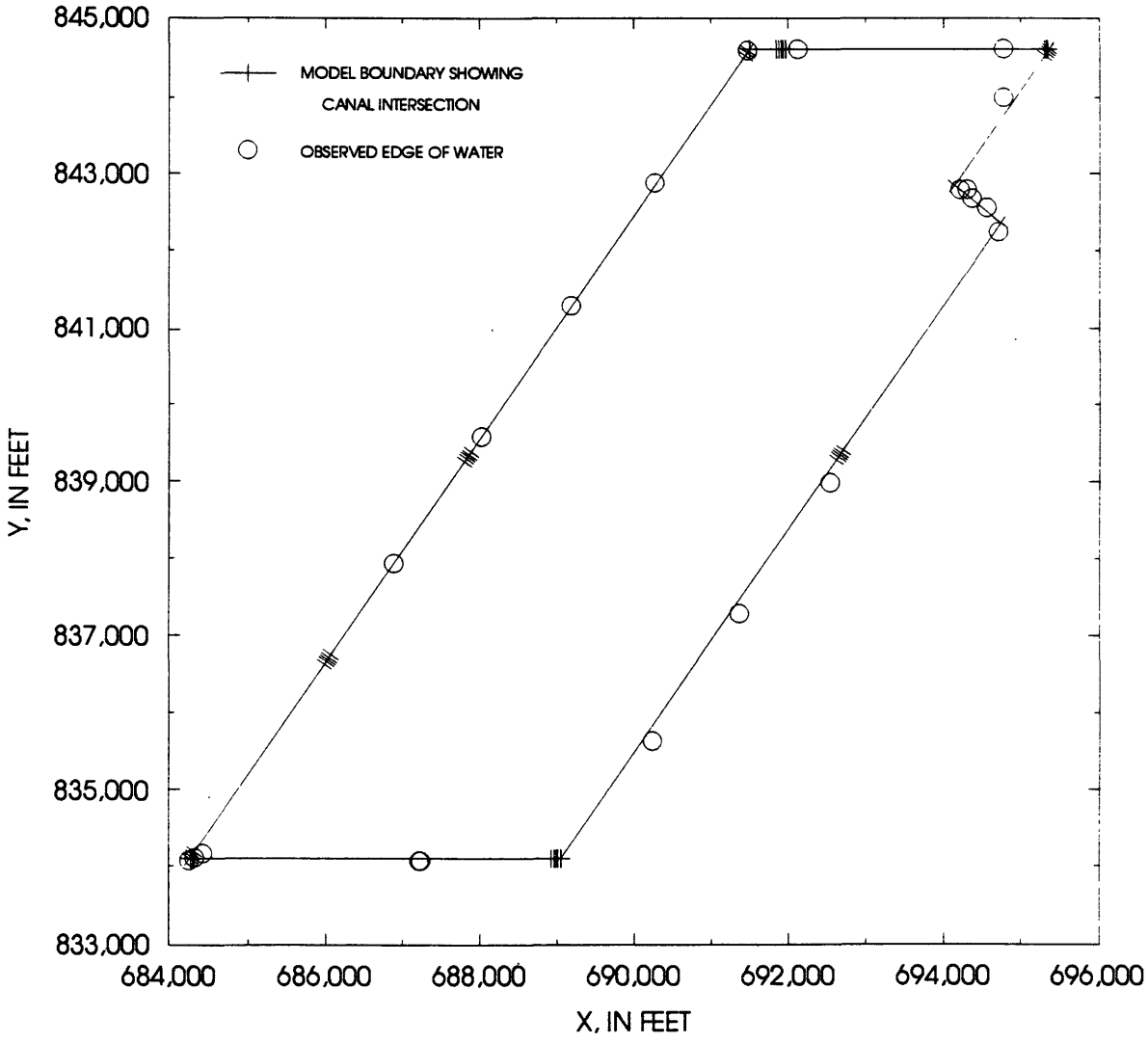

Figure 8: Model boundary of Cell 1 of the Everglades Nutrient Removal Project.

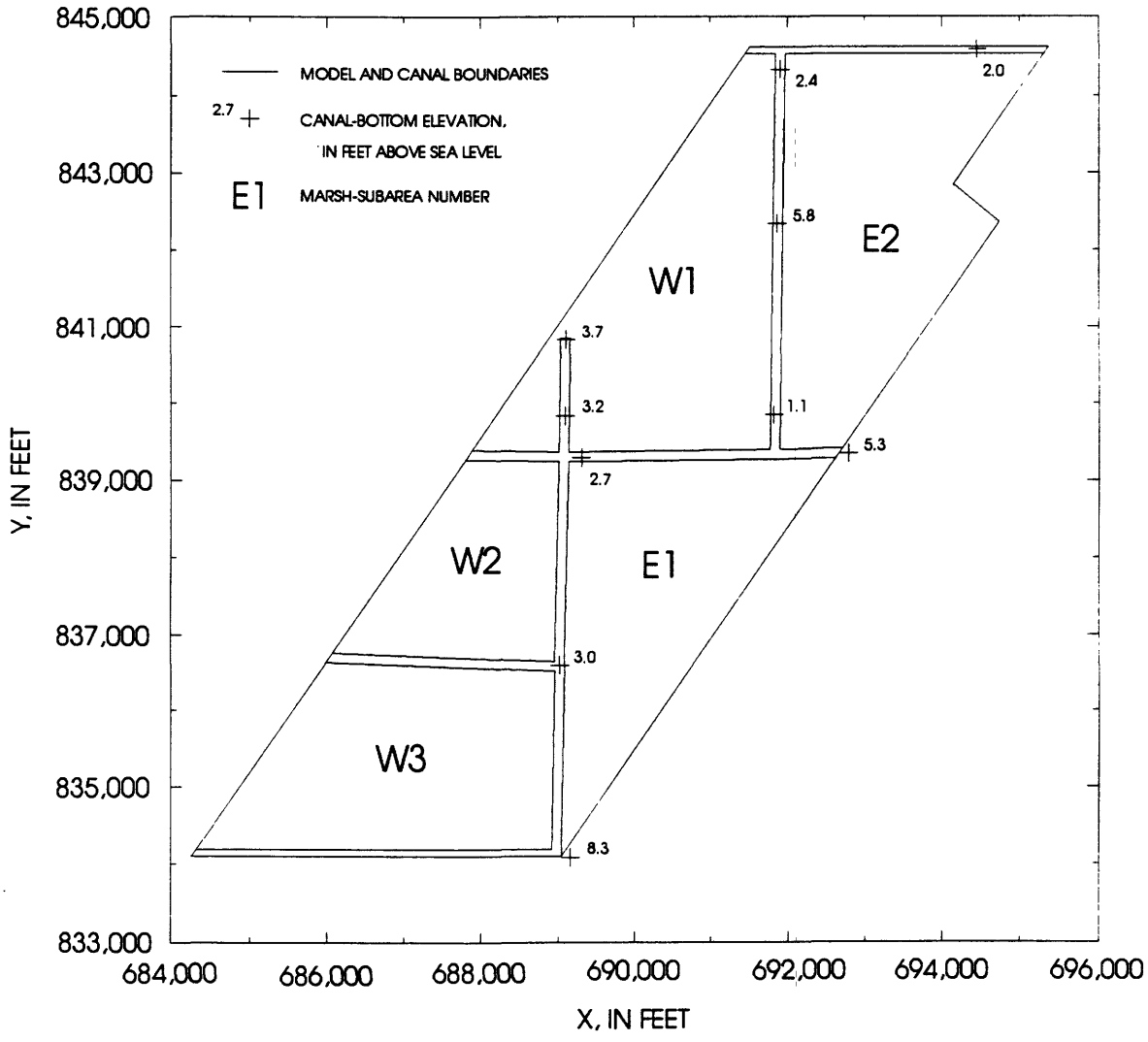

Figure 9: Boundaries of the canal-berm system and canal-bottom elevations in Cell 1 of the Everglades Nutrient Removal Project.

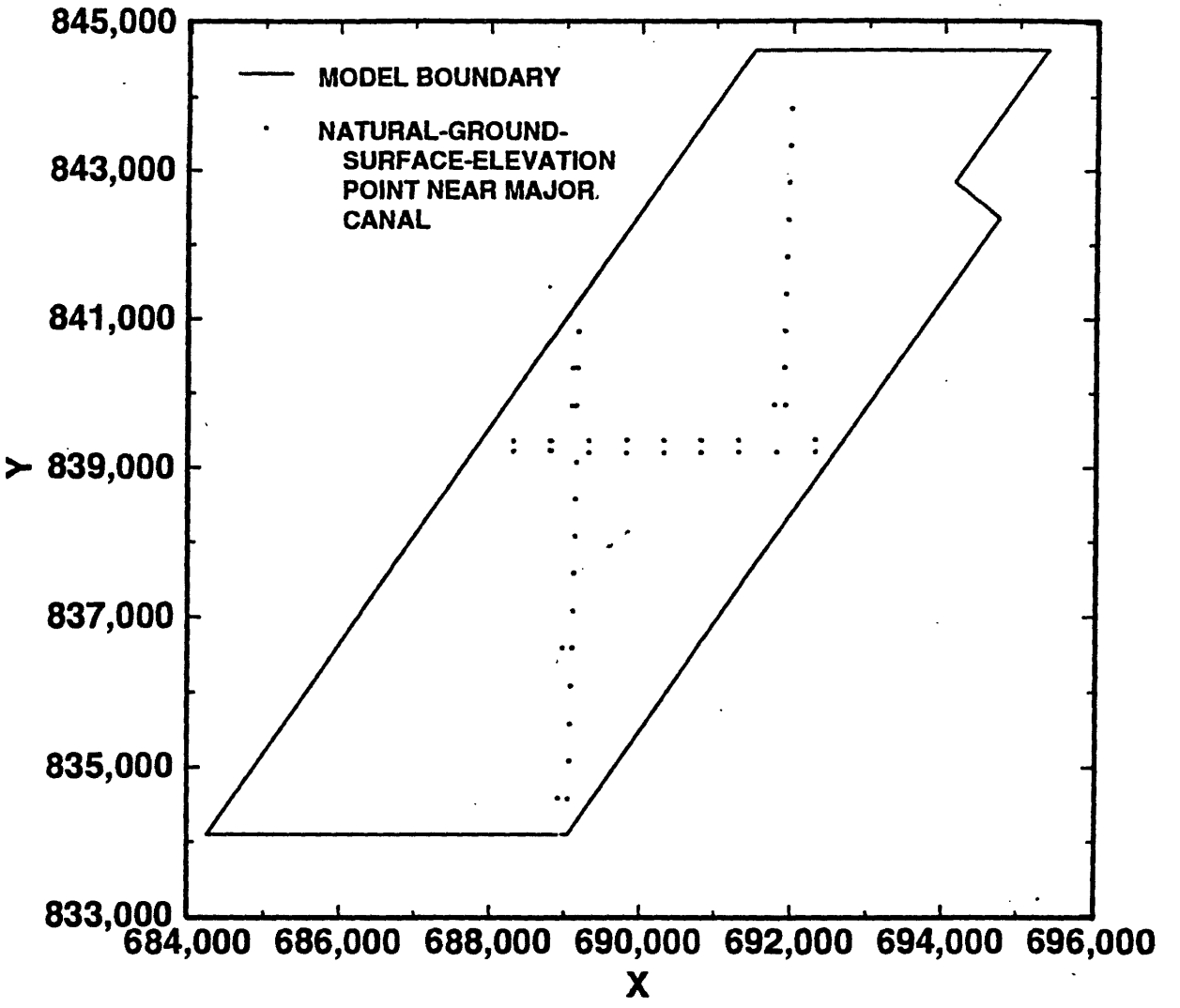

Figure 10: Natural-ground-surface-elevation points near major canals of Cell 1 of the Everglades Nutrient Removal Project.

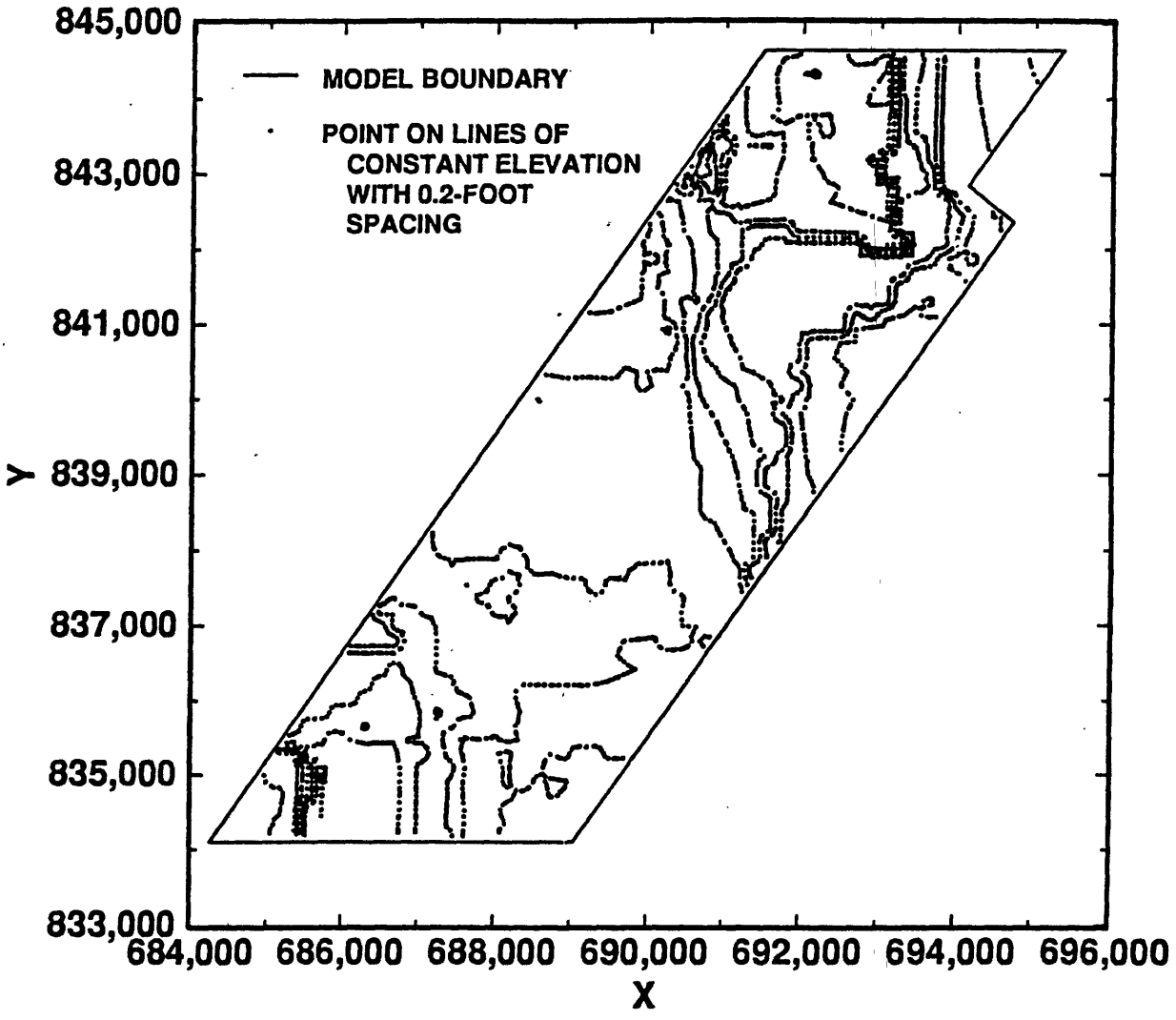

Figure 11: Points on lines of constant elevation with 0.2-foot spacing in Cell 1 of the Everglades Nutrient Removal Project.

Figure 12: Boundary and interior points used to interpolate ground-surface elevations in Cell 1 of the Everglades Nutrient Removal Project.

to both original and newly interpolated boundary points on the basis of the elevation data in DS-3 and DS-4. The final set of interior and boundary points is shown in figure 12.

For creating a finite-element grid from a set of points, TRIGRID requires that the origin of the coordinate system be near the area to be modeled. To accomplish this, the value 684,000 ft was subtracted from all x-coordinates and the value 834,000 ft was subtracted from all y-coordinates. This was done also during the creation of subsequent grids in the modeling process. TRIGRID was used to create a grid of triangles from the complete set of boundary and interior points. Several elements in the grid were modified to better represent the ground surface of Cell 1. The final ground-surface-interpolation grid is shown in figure 13.

The Model Grid for the Canal-Berm System

The model grid for the canal-berm system was designed first. The coordinates of corners of the canal-berm system were recorded, together with the coordinates of points where canal bottoms and the tops of canal banks met the model boundary. If the end of a canal reach was not perpendicular to its sides, then the projection of the intersection points on the sides of the reach also was recorded. This was done so that points on opposite sides of straight canal reaches were directly across from each other during subsequent insertion of intermediate points. The points determined in this way for the northwest part of Cell 1 are shown in figure 14. An aspect ratio of approximately 2:1 was selected for use with elements used to represent the triangular cross section of the canals. The choice of aspect ratio was made by balancing the need to minimize computation time by using as few elements as possible, the need to avoid long, narrow elements, which can cause numerical problems, and the need to have enough grid detail to be able to represent canal plugs. Thus, canal elements have a dimension of 25 ft perpendicular to a canal reach and a dimension of about 50 ft parallel to the canal reach. TRIGRID was used to interpolate points on straight segments of the canal-berm-system boundary so that points on opposite sides of a canal reach were positioned directly opposite each another. Nodes added in this way were located about 50 ft apart.

Interior points were added at canal junctions and angles to provide grid detail at these locations, and interior points were interpolated along the canal bottom and at the top of the bank along each straight canal reach. These

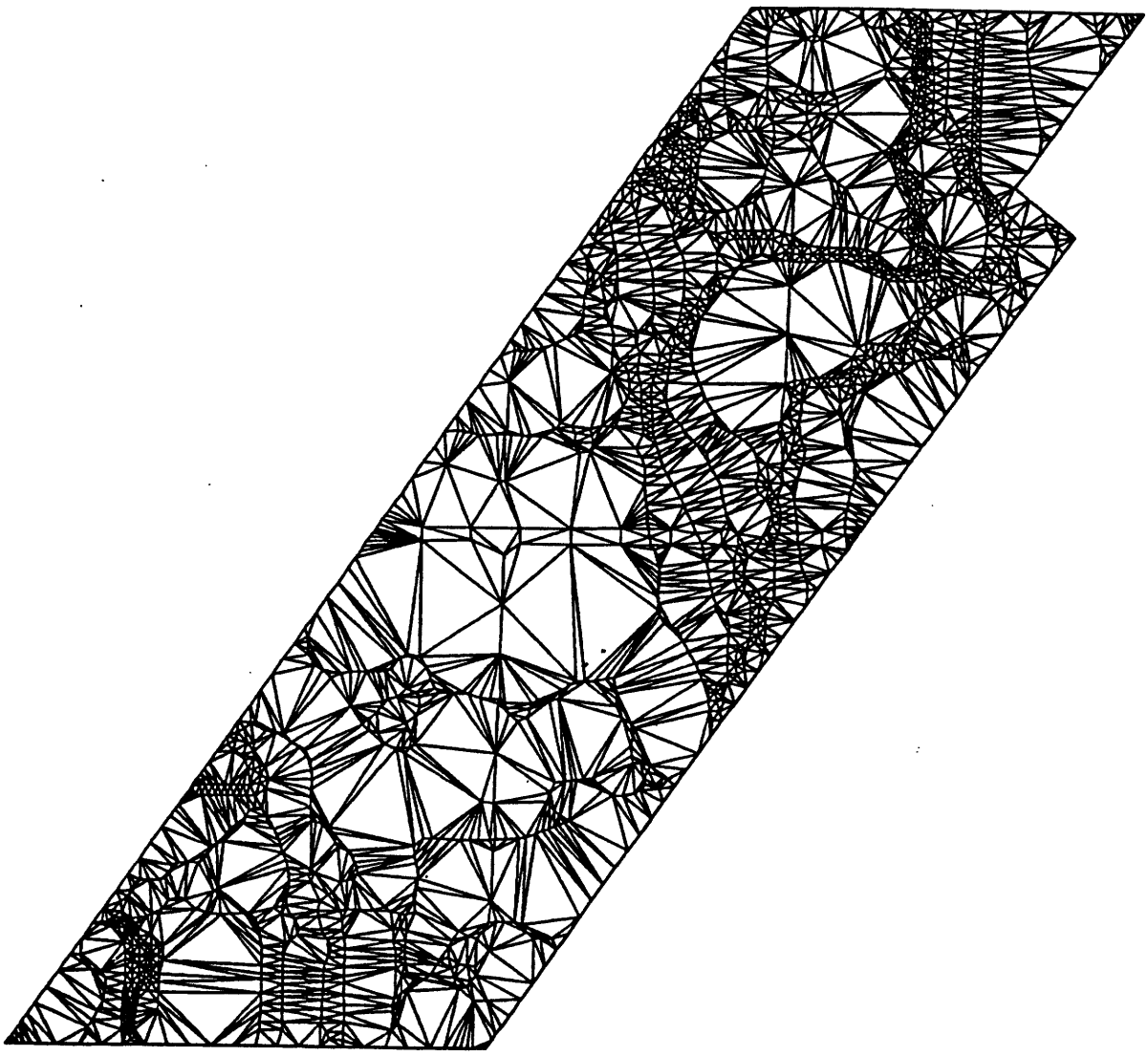

Figure 13: Ground-surface-interpolation grid for Cell 1 of the Everglades Nutrient Removal Project.

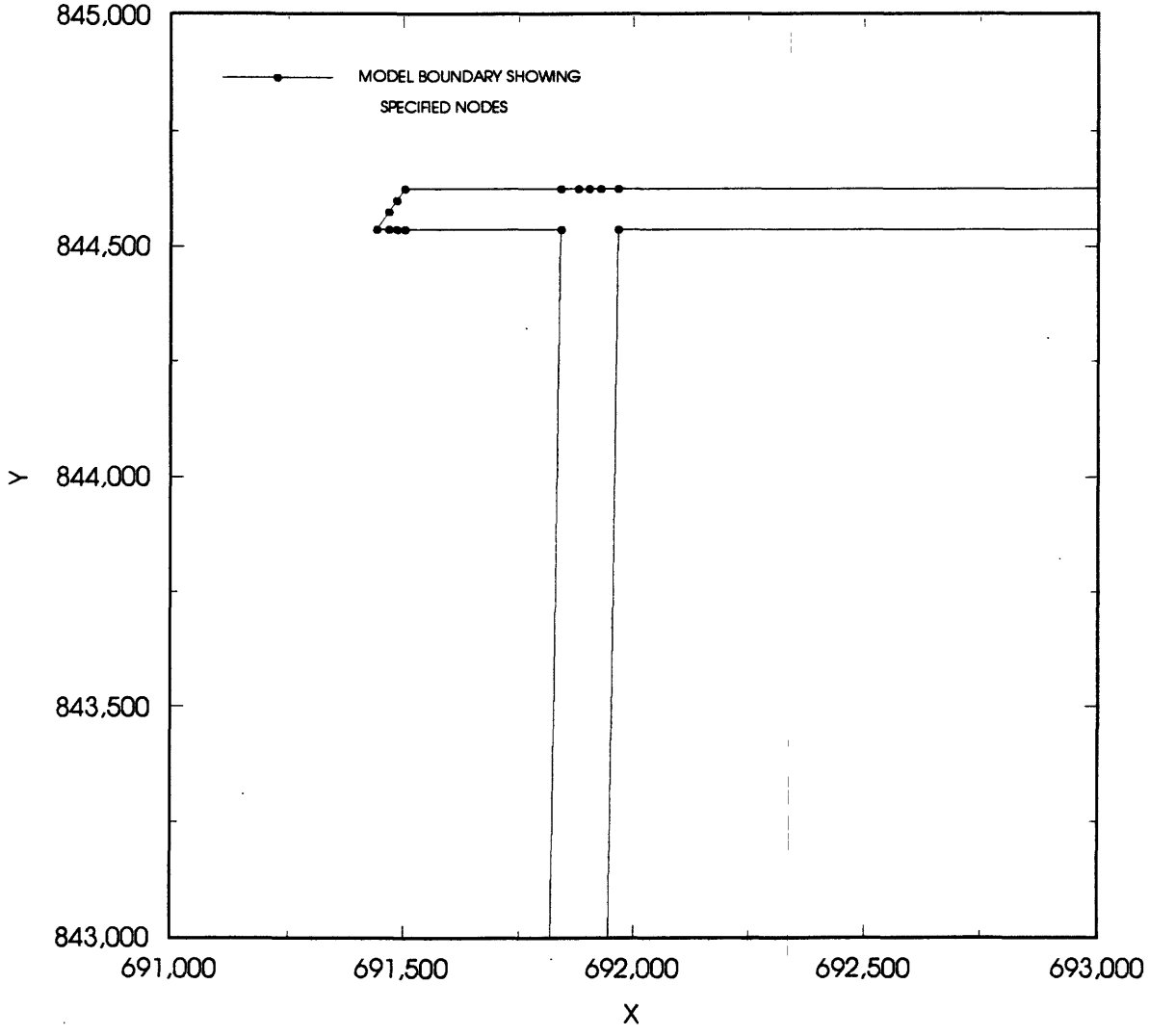

Figure 14: Specified points on the boundary of the northwest part of the canal-berm system in Cell 1 of the Everglades Nutrient Removal Project.

points were located about 50 ft apart and were aligned with points on the boundaries of the canal reach. To represent the canal-berm system with this amount of detail required 2,670 boundary and interior points. The complete set of points in the northwest part of the canal-berm system is shown in figure 15.

A model grid for the canal-berm system was created by applying the gridding feature of TRIGRID to the points generated for the system. During visual inspection of the grid, several unnecessary points were removed from the system. In a few cases, an element side between two triangular elements was shifted to improve the representation of the canal system. Several long, narrow, spurious triangles were removed along straight boundary segments of the grid. Codes were assigned to the 2,670 points of the canal-berm-system grid to ensure that they remained stationary during subsequent operations on the complete Cell 1 grid. The final model grid for the northwest part of the canal-berm system is shown in figure 16.

Model Grids for Marsh Subareas

TRIGRID was used to create model grids for each of five marsh subareas of Cell 1. These five subareas are denoted by E1, E2, W1, W2, and W3 and are shown in figure 9. In each case the same steps were followed to create the grid.

Consider, for example, subarea E1. The boundary points of E1 are the points in common with the canal-berm-system boundary and the appropriate subset of points belonging to the boundary of the ground-surface-interpolation grid for Cell 1 (fig. 12). To generate a model grid for E1, with a smooth transition from small elements near the canal-berm system to large elements far from the canals, the node-density scaling feature of TRIGRID was used. This feature uses a scaling variable and a quadratic polynomial function of that variable. The scaling variable is defined at both boundary and interior points of a coarse scaling grid, which is created solely for the purpose of assigning model node density.

To create the scaling grid for E1, the points on the boundary of the E1 model grid were replaced with a set of fewer points. Interior points were added manually. The scaling variable was assigned the value 10.0 at points on and near the canal-berm system and at points on the external boundary near an intersection with a canal. The value 1.0 was assigned to the variable at points on the external boundary far from canals. Intermediate values were

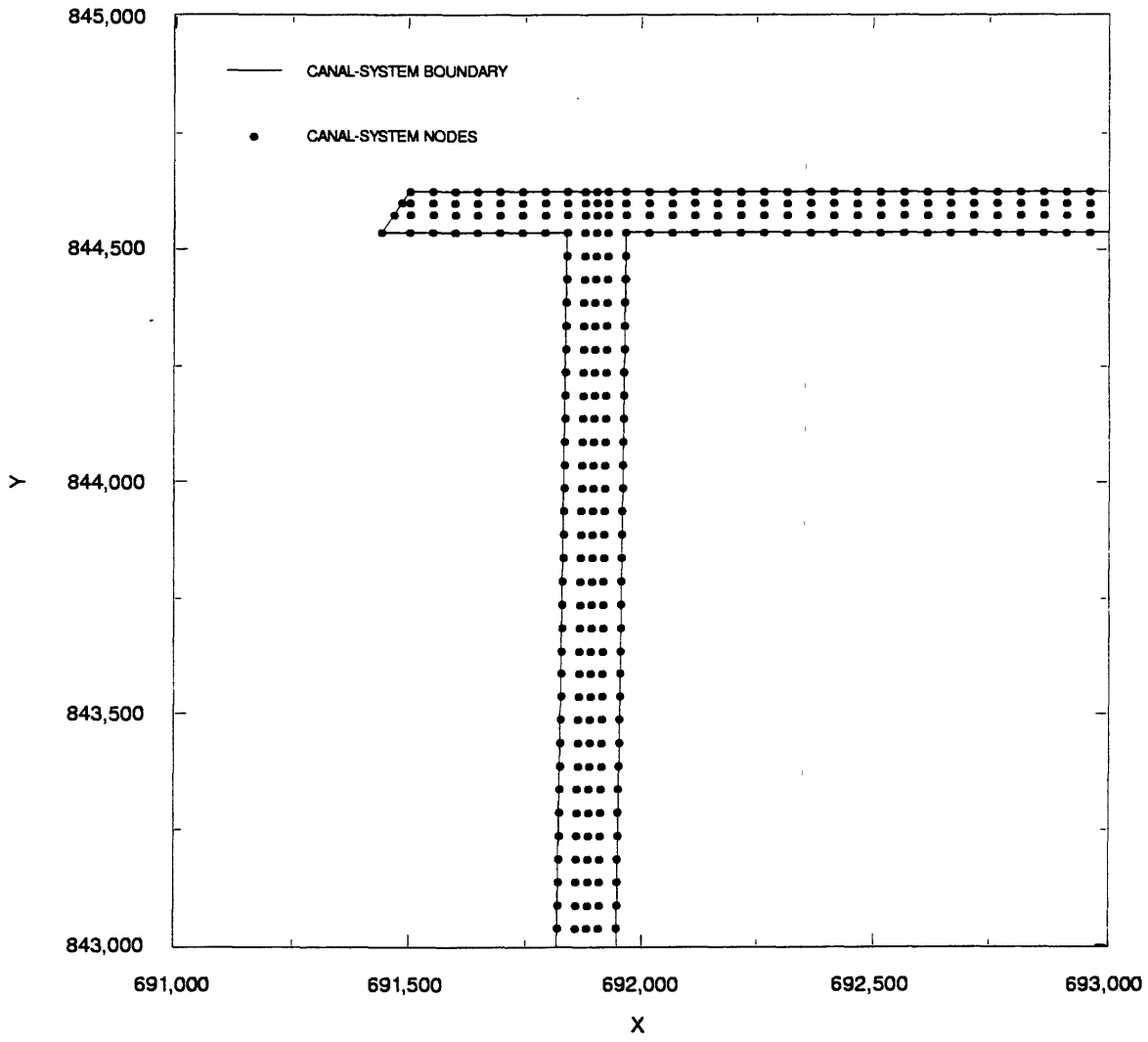

Figure 15: Node points on the boundary and in the interior of the northwest part of the canal-berm system in Cell 1 of the Everglades Nutrient Removal Project.

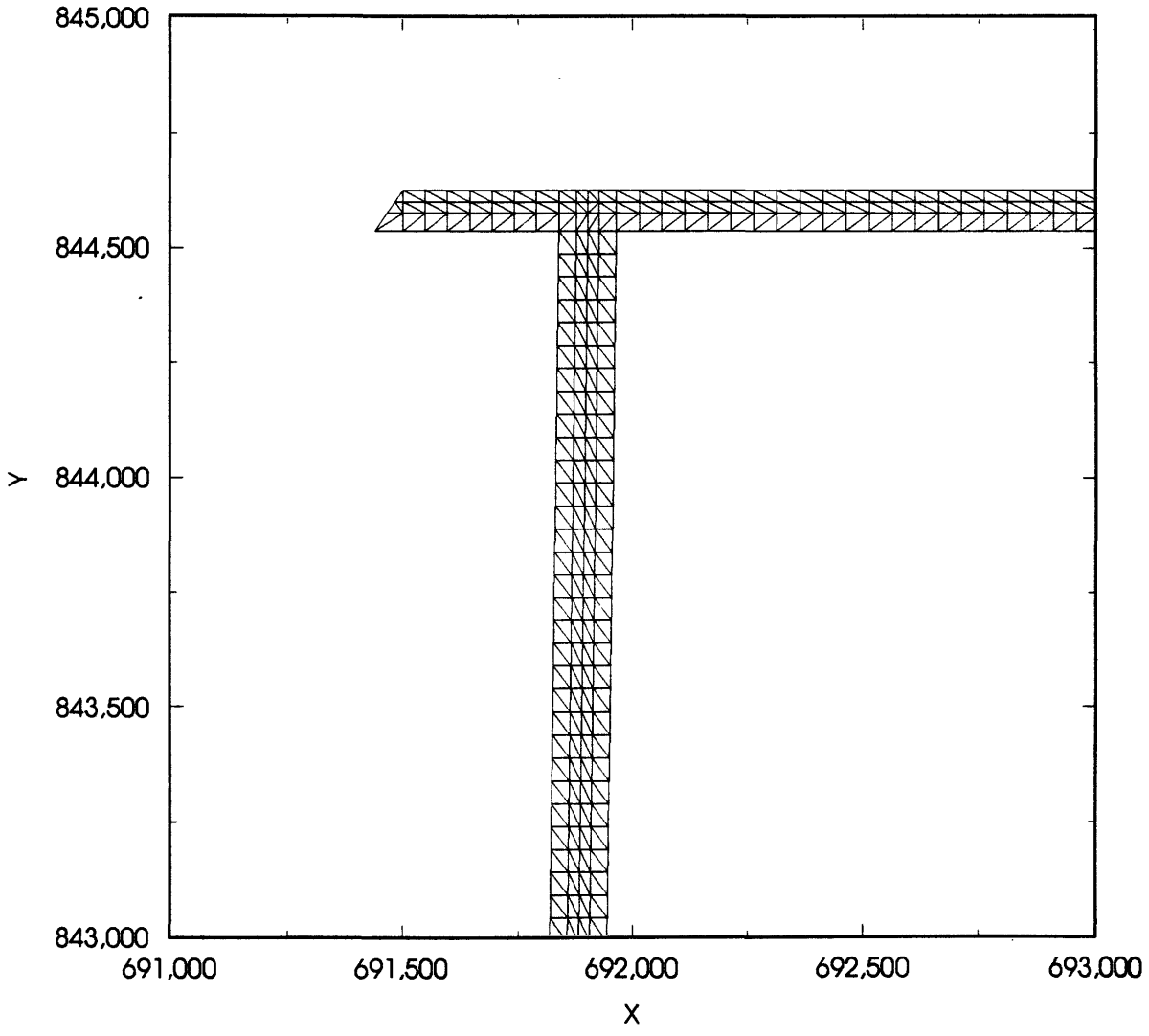

Figure 16: Model grid for the northwest part of the canal-berm system in Cell 1 of the Everglades Nutrient Removal Project.

assigned to intermediate points. The gridding feature of TRIGRID was used to create a scaling grid from the coarse set of points. A few element sides were exchanged, and a few spurious elements were removed. The final scaling grid for area E1 is shown in figure 17.

To create a set of interior model points from a set of boundary points and a scaling grid, TRIGRID lays a fine square mesh over the model domain (Walters and Henry, 1997). For E1, a square mesh size of 25 ft was selected. For this mesh size and the definition of the scaling variable, s, the scaling function

$$a_0 + a_1 s + a_2 s^2 \tag{36}$$

was found by trial and error to give a model node set with a smooth transition in node spacing for coefficient choices $a_0 = 117.333$, $a_1 = -18.0$, and $a_2 = 0.667$. Then a model grid was created from the model node set, and a few spurious elements were removed. The unsmoothed model grid for area E1 is shown in figure 18. The same procedure used to create the model grid for area E1 was used to create model grids for areas E2, W1, W2, and W3.

The Model Grid for Cell 1

The model grid for the canal-berm system and the model grids for marsh areas E1, E2, W1, W2, and W3 were merged by applying the grid-joining function of TRIGRID. The combined grid had 5,384 nodes and 10,412 triangular elements. The merged grid was smoothed. During smoothing, canal-berm-system and boundary nodes were not moved. The final, smoothed grid is shown in figure 19. The ground-surface-interpolation grid was used to interpolate natural ground-surface elevations throughout Cell 1. Lines of constant model ground-surface elevation (excluding the canal-berm system) are shown in figure 20.

From ground-surface elevations in data set DS-3, it was determined that there are low berms on the east side of canal reach AH, the north side of canal reach FI, and the west side of canal reach GM (fig. 21). The average berm heights were 0.53 ft for reach AH, 0.9 ft for reach FI, and 0.6 ft for reach GM. The elevations for the appropriate canal banks in the model were increased by these amounts. On the basis of canal-bottom elevations in data set DS-3, shown in figure 9, model canal-bottom elevations were set to 2.0 ft above sea level for canal reach AC, 3.1 ft above sea level for reach AH, 3.4 ft above sea level for reach EG, 2.7 ft above sea level for reach FI, and

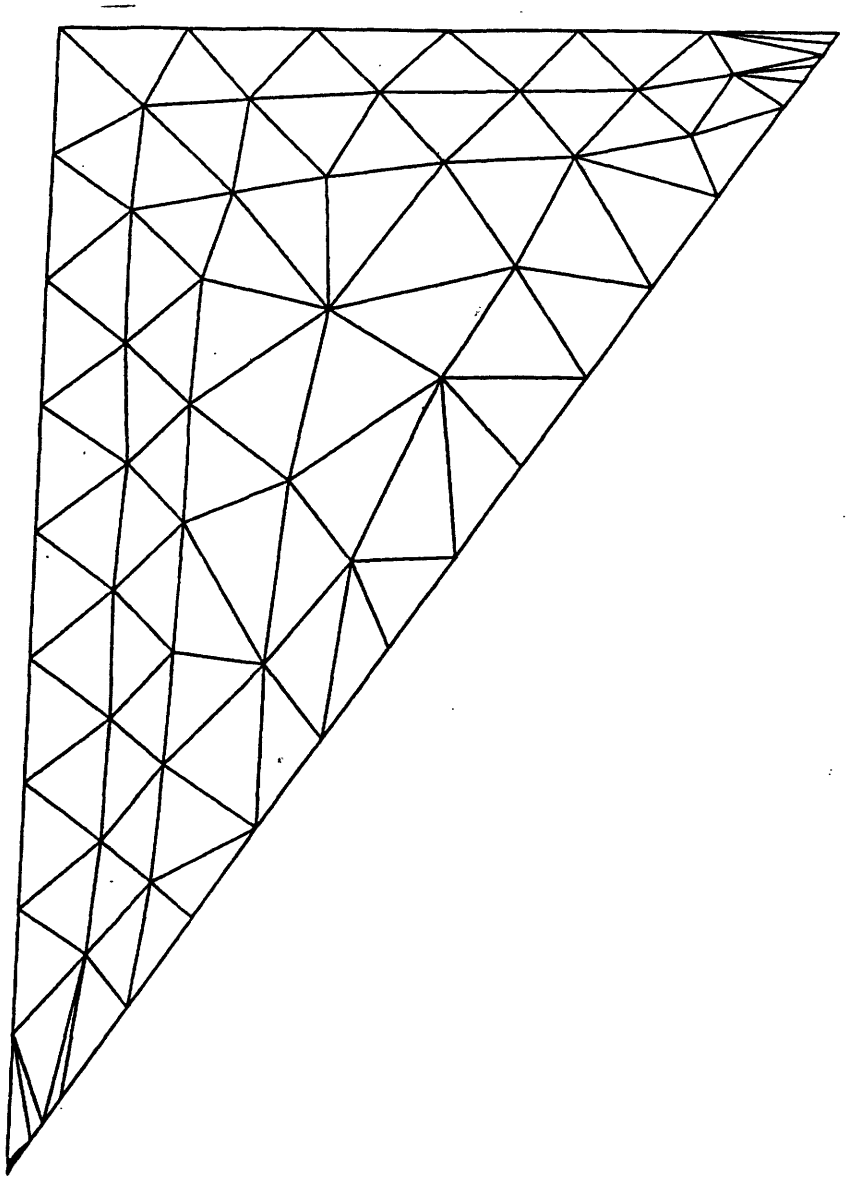

Figure 17: Coarse scaling grid used to determine model node density in area E1 of the Everglades Nutrient Removal Project.

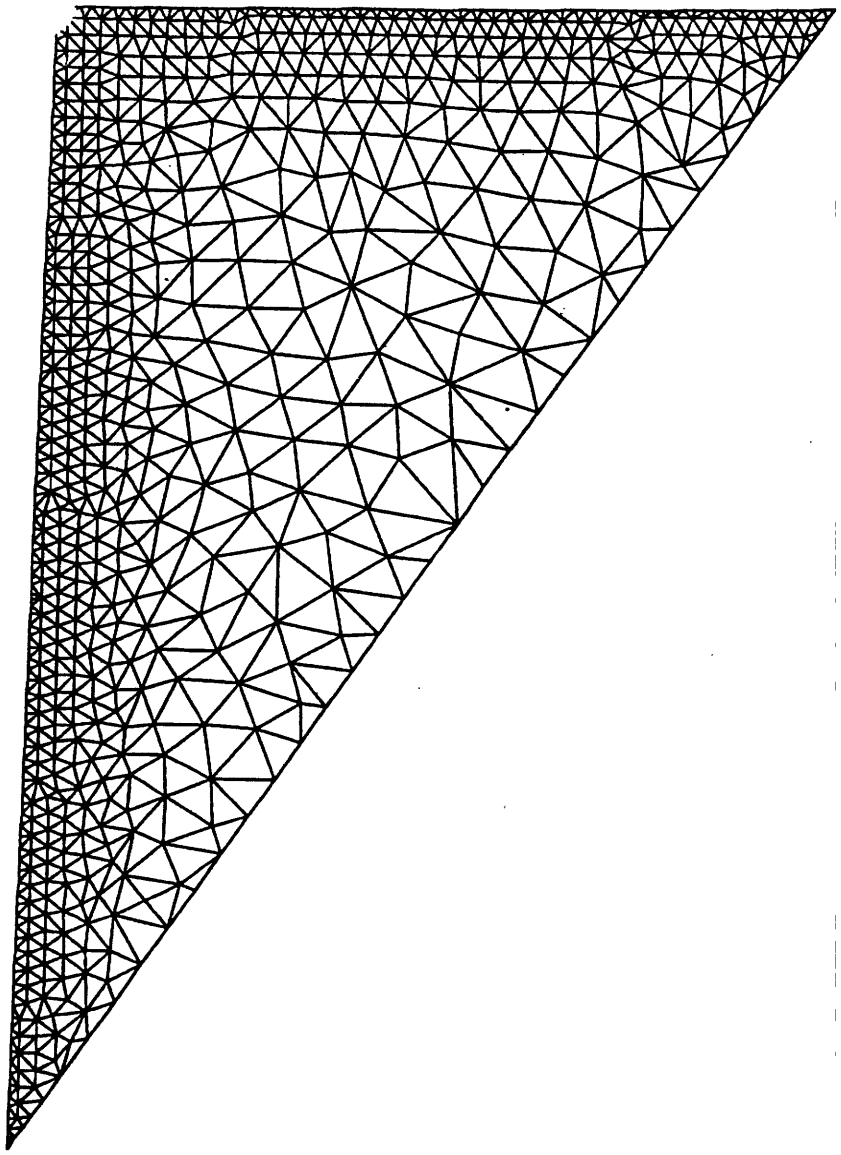

Figure 18: Unsmoothed model grid for area E1 of the Everglades Nutrient Removal Project.

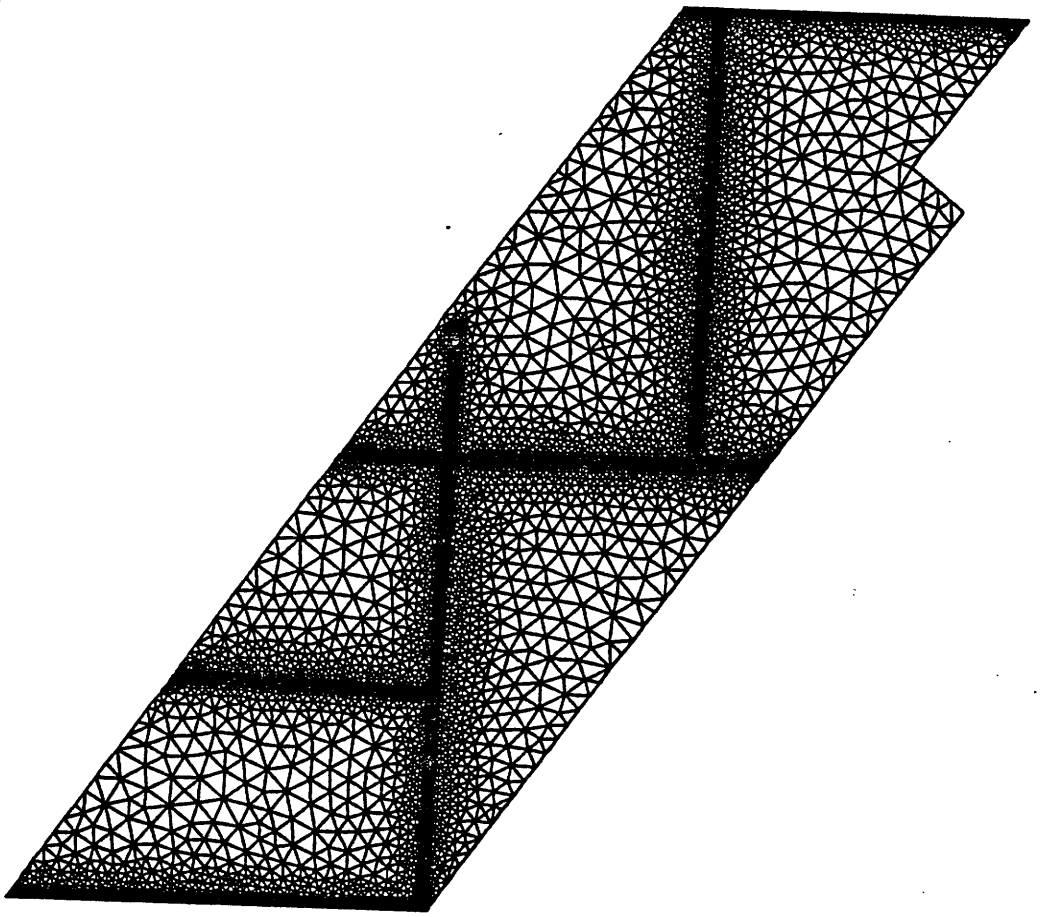

Figure 19: Smoothed model grid for Cell 1 of the Everglades Nutrient Removal Project.

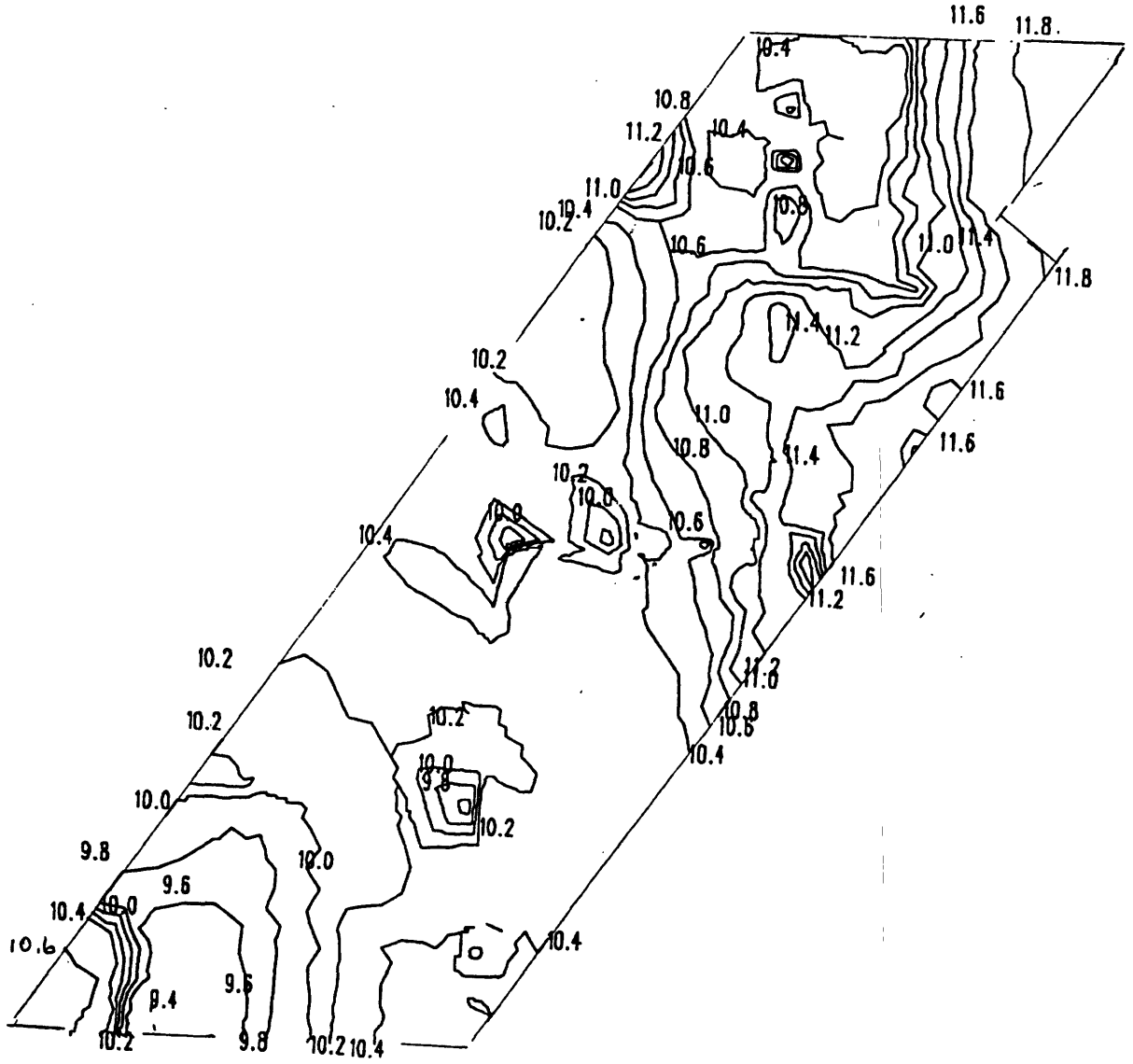

Figure 20: Lines of constant ground-surface elevation for Cell 1 of the Everglades Nutrient Removal Project.

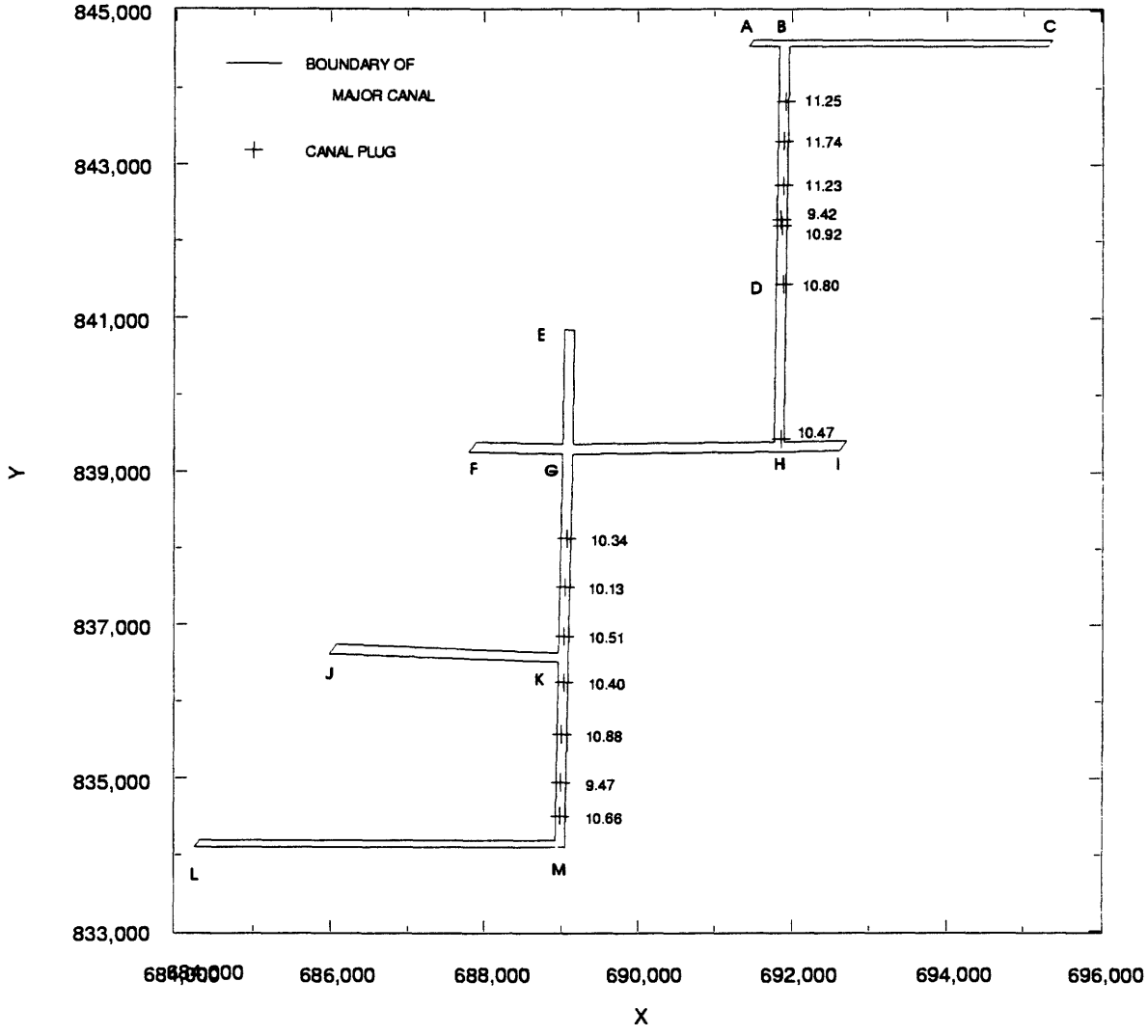

Figure 21: Locations and elevations of canal plugs in Cell 1 of the Everglades Nutrient Removal Project.

5.7 ft above sea level for reach GM. No information was available for reaches JK and LM; canal-bottom elevations there were set to 6.0 ft above sea level. Fourteen plugs are present in the north-south reaches of the canal system. The locations and elevations of the plugs are shown in figure 21. To represent the plugs in the model, the elevation of the node closest to each plug was set to the plug elevation. At the time of the survey of the plug elevations, it was noted that the canal reach between the southernmost two plugs on canal reach AH had partially filled in. Consequently, the canal-bottom elevation was set to 9 ft above sea level between the two plugs.

To assign codes to triangles to represent vegetation parameters (used to determine the sheltering of the water surface from wind) and flow resistance due to bed friction and vegetative drag, TRIGRID was used to create polygons that enclosed subreaches of the canal system and large areas of cattails and mixed vegetation. The polygons for cattails and mixed vegetation were based on the October 14, 1994, vegetation map of the ENR Project (South Florida Water Management District, 1994) and are shown in figure 22. TRIGRID was used to assign appropriate triangle codes to triangles within each polygon.

TRIGRID was then used to reorder the triangles in the grid to reduce solution time during model runs. Finally, a TRIGRID program was used to convert the three-node triangular elements into six-node triangular elements required by the flow model. The final model grid had 21,179 nodes and 10,412 triangular elements. A computer program was written and used to convert the single code assigned to each element by TRIGRID into a series of codes to define the turbulence, friction, vegetation, precipitation, evapotranspiration, and ground-water inflow/outflow characteristics of each element.

Model Implementation and Calibration

Data from the 5-day period March 17–21, 1996, were selected for use in calibrating the model. During this period, mean daily inflows and outflows, as well as water-surface elevations throughout Cell 1, varied little. Thus, the assumption of steady flow is reasonable.

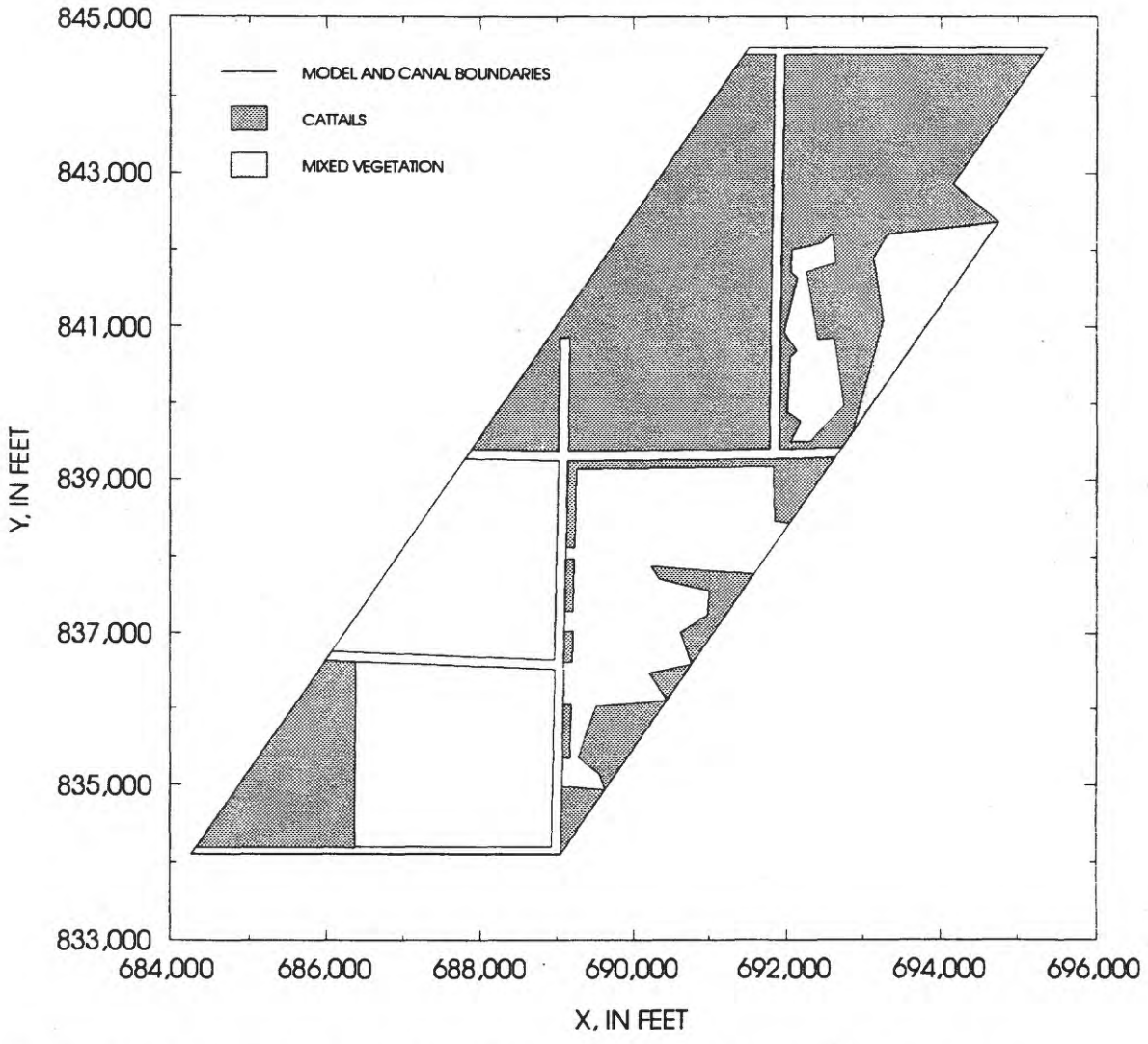

Figure 22: Polygons enclosing areas of cattails, mixed vegetation, and open water in Cell 1 of the Everglades Nutrient Removal Project.

Model Implementation

The mean and standard deviation of flows at the 10 inflow and 10 outflow culverts are given in table 1. Water-surface-elevation data at the upstream and downstream ends of Cell 1, at station ENR101 at the center of Cell 1, and at the upstream end of Cell 3 are given in table 2. All these sites are shown in figure 3.

Table 1. Cell 1 inflows and outflows for March 17–21, 1996.

Culvert number	Mean discharge, in cubic feet per second	Standard deviation, in cubic feet per second
G-252A	50.2	6.71
G-252B	43.2	6.71
G-252C	36.8	5.80
G-252D	34.6	5.84
G-252E	35.0	5.36
G-252F	37.2	5.63
G-252G	33.0	5.56
G-252H	29.8	4.40
G-252I	25.8	3.77
G-252J	26.3	4.27
G-253A	42.3	5.60
G-253B	39.4	4.72
G-253C	38.3	4.39
G-253D	42.0	4.92
G-253E	28.0	4.54
G-253F	26.4	4.14
G-253G	37.4	5.17
G-253H	22.4	4.50
G-253I	35.8	3.45
G-253J	31.2	2.93

Table 2. Cell 1 water-surface elevations for March 17–21, 1996.

Station number	Mean water-surface elevation, in feet above sea level	Standard deviation, in feet
G-252AB$_T$	12.72	0 .03
G-252EF$_T$	12.78	.04
G-252IJ$_T$	12.80	.04
G-253AB$_H$	12.50	.03
G-253AB$_T$	12.43	.03
G-253EF$_H$	12.54	.03
G-253EF$_T$	12.45	.02
G-253IJ$_H$	12.55	.03
G-253IJ$_T$	12.51	.03
ENR101	12.60	.02

In the model, inflow at each culvert G-252A through G-252J was treated as flow normal to the model boundary at the element-midside node closest to the location of the corresponding culvert. Flows at culverts G-252I and G-252J were combined at a single node because of the omission of a section of the upstream boundary of Cell 1 near the group of 15 test cells. All other boundaries were treated as zero-normal-flow (slip) boundaries.

At the downstream end, culvert flow (equations 20 and 21) was simulated between Cells 1 and 3 at structures G-253A through G-253J. Tail-water elevations, z_s^t, were interpolated from water-surface elevations at stations G-253AB$_T$, G-253EF$_T$, and G-253IJ$_T$. The culvert discharge coefficients, C_c, were adjusted during model calibration to give the correct flows at the culverts. The remaining parameters were assigned the same values for all 10 culverts: $A_c = 28.27$ ft^2, $R_c = 1.5$ ft, $L_c = 50$ ft, and $n_c = 0.022$. It was assumed that the culverts were fully submerged.

Twenty levee segments were used along the boundary between Cell 1 and WCA-1 to simulate seepage into Cell 1 both through and under the L-7 levee (equations 26 and 35). The regression equations developed by Guardo (1996) and Prymas (1997) to express surficial seepage through the L-7 levee and subsurface seepage under the levee from WCA-1 into the ENR Project as a function of water-surface elevations in WCA-1 and the project were used to obtain daily seepage rates. Daily surficial-seepage rates through the entire 5-mile-long levee were calculated as 3.97, 3.98, 3.58, 3.55, and 3.33 ft^3/s for each of the 5 days, March 17–21, 1996. Subsurface seepage rates were calculated as 18.29, 18.32, 17.92, 18.09, and 17.95 ft^3/s for the 5-day period. Because 48.4 percent of the L-7 levee forms part of the boundary of Cell 1, the average seepage through the levee into Cell 1 was estimated to be 1.78 ft^3/s, and the average seepage under the levee was estimated to be 8.78 ft^3/s for the 5-day period. The permeabilities, k_t and k_u, of levee segments and levee-segment sublayers were assumed to be the same for all segments and were adjusted during model calibration to give the correct total flows through and under that part of the levee adjoining Cell 1. The remaining parameter values were taken to be the same for all levee segments: $z_b + H_1 = 16.35$ ft, $b_2 = 102$ ft, $b_1 = 30$ ft, $h_\ell = 12$ ft, $L_\ell = 600$ ft, and $D = 50$ ft. Here, $z_b + H_1$ is the mean water-surface elevation in WCA-1, and L_ℓ is the length of the levee segments. The thickness, D, of the permeable sublayer, was calculated on the basis of the work of Prymas (1997).

Precipitation, evapotranspiration, and ground-water inflow/outflow were accounted for in the model. The rainfall for the period, 0.15 in, was obtained

from the rain gage at station ENR101 (fig. 3) and treated as spatially constant within Cell 1. An equivalent, constant rate, $q_p = 0.00145$ in/h, for the model area was used in the steady-state simulation. This rate was obtained from the constant rate, 0.00125 in/h, for the 1,297 acres of Cell 1 by multiplying by 1.162, the ratio of the physical size of the cell to the model size, 1,116 acres. A steady, spatially constant evapotranspiration rate, $q_e = 0.174$ in/d, for the model area was estimated from daily losses of 0.153, 0.174, 0.123, 0.164, and 0.138 in. during the 5-day period. This rate also was obtained by multiplying the rate for the actual cell, 0.150 in/d, by the factor 1.162.

A mass balance for Cell 1 was used to estimate the outflow of surface water to ground water. The sum of the 10 mean inflows for the period March 17–21, 1996, is 351.7 ft^3/s, and the sum of the 10 mean outflows is 343.2 ft^3/s. Seepage through and under the levee from WCA-1 into Cell 1 was estimated to be 10.6 ft^3/s. The surface area of the Cell 1 model is 4.86×10^7 ft^2. Thus, the precipitation rate of 0.00145 in/h corresponds to an inflow of 1.6 ft^3/s, and the evapotranspiration rate of 0.174 in/d corresponds to an outflow of 8.2 ft^3/s. Subtracting outflow and evapotranspiration from inflow, levee seepage, and precipitation gives 12.5 ft^3/s, which was assumed to be flow from surface water to ground water. Dividing this flow rate by the model area of Cell 1 gives $q_g = 0.267$ in/d. For this simulation, z_g was assumed to be 12 ft above sea level. Therefore, the first part of equation 19 was valid. The thickness, M_ℓ, of the low-permeability layer was assumed to be 10 ft, the sum of the thickness of the limestone cap rock, about 5 ft, and the thickness of the peat layer above it, also about 5 ft. To obtain an initial estimate of the hydraulic conductance, C_ℓ, it was assumed that the water-surface elevation, $z_b + H$, was approximately 12.6 ft above sea level. Then, from equation 19, the conductance was estimated to be $4.30 \times 10^{-7}/s$. This value was used as the initial estimate of C_ℓ in the model.

Flow resistance due to bed roughness and vegetative drag, wind, and turbulent stresses also were accounted for in the model. The eddy-viscosity coefficients, $\hat{\nu}_0$ and c_μ, were assigned the values 1.0 ft^2/s and 0.6, respectively. Momentum-correction coefficients were assigned the value 1.0. During development of the grid, unique friction codes were assigned to elements representing canal bottoms and areas of cattails, mixed vegetation, and shallow open water with submersed vegetation. Unique friction codes also were assigned to elements representing the partially filled area in the southern part of canal AH (fig. 21) and to one row of elements upstream and downstream from each canal plug. The values of the roughness coefficients that apply

to these groups of elements were adjusted during model calibration to make the difference between observed and computed discharges, velocities, and water-surface elevations as small as possible.

Hourly wind data were available from weather station ENR105 (fig. 3). The mean wind speed for the period from March 17 to 21, 1996, was 18.2 ft/s, with a standard deviation of 8.3 ft/s. The mean direction from which the wind was blowing was 231 degrees (clockwise from north), with a standard deviation of 61 degrees. Constant wind speed and direction given by the mean values were used in the model. (The flow model requires as input the direction, ψ, toward which the wind is blowing, measured counterclockwise from the positive x-axis (east). Consequently, the direction, ψ, used in the model was 39 degrees.) The surface-stress coefficient, c_s, was assigned the value 1.0. Because the model accounts for the reduction of surface shear stress by emergent vegetation (equation 9), vegetation characteristics were estimated for cattails, mixed vegetation, and open water with submersed vegetation. For open water, $N_v = 0.2$ stems/ft^2, $w_v = 0.05$ ft, and $h_v = 1$ ft. Because of the small value used for plant height, h_v, there was almost no sheltering effect in open water. For both cattails and mixed vegetation, $N_v = 4$ stems/ft^2, $w_v = 0.05$ ft, and $h_v = 8$ ft. Consequently, in areas dominated by cattails and mixed vegetation, the surface stress was negligible. The vegetative drag coefficient, c_v, was set equal to 1.0 in all three cases.

Additional Calibration Data

Additional data were obtained for use in calibrating the model. At 11:10 a.m. on March 22, 1996, an electromagnetic current meter was used to obtain a velocity profile at the fifth plug from the north end of canal reach BH (fig. 21). The elevation of the plug is 10.9 ft above sea level, and velocities 0.09, 0.25, and 0.37 ft/s were recorded at distances 0.25, 0.75, and 1.0 ft below the water surface, respectively. A dense growth of water hyacinths was observed in the channel just upstream from the measurement site. This measurement was made on the day after the 5 days, March 17–21, of relatively steady flow. The mean total inflow at culverts G-252A through G-252J on March 22 was 231 ft^3/s (66 percent of the mean inflow for March 17–21) and the mean total outflow at culverts G-253A through G-253J was 324 ft^3/s (94 percent of the mean outflow for March 17–21).

A dye release was made on April 4, 1996, at station ENR101. Six autosamplers were installed before the release in two east-west transects 819

and 1,462 ft south of the release location. In each transect, the center autosampler was due south of the release point, and the other two were about 200 ft due east and west of the center one. The dye was released at 9 a.m., April 4. The largest dye concentrations were observed at the western sampler in each transect. The peak concentration was observed about 6 h after release at the first transect and about 20 h after release at the second transect. Because the concentration peaks were observed at the westernmost samplers, it was considered possible that the center of mass of the dye cloud passed west of the samplers. The distance from the dye-release point to the western sampler in the first transect was 844 ft, and the distance from the release point to the western sampler in the second transect was 1,489 ft. Consequently, the mean speed and direction of dye traveling from station ENR101 to the two western samplers were 0.039 ft/s and 194 degrees (clockwise from north) for the first transect and 0.021 ft/s and 188 degrees for the second transect. Mean total Cell 1 inflows at culverts G-252A through G-252J were 331 ft^3/s on April 4 and 200 ft^3/s on April 5 (94 and 57 percent, respectively, of the mean inflow for March 17–21). Mean total outflows at culverts G-253A through G-253J were 225 ft^3/s and 241 ft^3/s (66 and 70 percent, respectively, of the mean outflow for March 17-21). The mean wind speed during the hours of the dye study was about 7.0 ft/s, and the mean wind direction was about 146 degrees. Although conditions were different from those on March 17–21, 1996, during both the profile measurement and the dye release, the information was considered useful in providing approximate values of velocity in the marsh and at a canal plug for consideration during model calibration.

Model Calibration

The first model iteration was made with a horizontal water surface of 13 ft above sea level and zero velocities assigned to all nodes. Inflows, outflows, levee seepage, precipitation, evapotranspiration, ground-water outflow, and wind were set as discussed above. The tail-water elevations at the 10 outflow culverts were set at 12.95 ft above sea level, slightly less than the initial headwater elevation of 13 ft above sea level. Reasonable values were assigned to Manning's n. During subsequent iterations, the tail-water elevations were reduced in increments of 0.05 ft to values interpolated from the Cell 3 water-surface elevations at stations G-253AB_T, G-253EF_T, and G-253IJ_T (table 2). The results of one iteration were used as initial conditions for the next

iteration. Then, during a large number of iterations, values of Manning's n, culvert discharge coefficients, hydraulic conductance, and levee permeabilities were adjusted until culvert outflows, water-surface elevations, and levee seepage matched observed data or independently calculated values.

For the calibrated model, the values of the outflow-culvert discharge coefficients giving computed culvert discharges at structures G-253A through G-253J within 1 percent of the measured discharges and computed water-surface elevations at stations G-253AB$_H$, G-253EF$_H$, and G-253IJ$_H$ within 0.02 ft of observed elevations are given in table 3, together with the computed discharges and culvert headwater elevations. Permeabilities of 93.3 and 48.7 ft/d gave seepage of 1.78 ft^3/s through the L-7 levee and seepage of 8.78 ft^3/s under the L-7 levee, respectively. The initial choice of the hydraulic conductance, 4.30×10^{-7}/s, resulted in mass-flux balance. Consequently, the hydraulic conductance was not changed.

Table 3. Measured and computed Cell 1 outflows, discharge coefficients, and computed headwater elevations at culverts G-253A through G-253J for March 17–21, 1996.

Culvert number	Measured discharge, in cubic feet per second	Computed discharge, in cubic feet per second	Discharge coefficient, dimensionless	Computed headwater elevation, in feet above sea level
G-253A	42.3	42.4	0 .67	12.52
G-253B	39.4	39.2	.62	12.52
G-253C	38.3	38.1	.60	12.53
G-253D	42.0	42.2	.68	12.53
G-253E	28.0	28.0	.43	12.53
G-253F	26.4	26.2	.42	12.54
G-253G	37.4	37.4	.70	12.54
G-253H	22.4	22.6	.45	12.54
G-253I	35.8	35.9	.93	12.54
G-253J	31.2	31.1	1 .00	12.54

Values of Manning's n of 0.18 for shallow open water with submersed vegetation and 0.27 for marsh with both cattails and mixed vegetation were found to result in close agreement between observed and computed water-surface elevations at stations G-252AB$_T$, G-252EF$_T$, G-252IJ$_T$, and ENR101, as shown in the column labeled "Run C" of table 4. The value of Manning's n for shallow open water was affected by the presence of submersed vegetation and sugar-cane stubble. The n value of 0.27 for marsh with cattails was affected by the presence of small ditches that were not included in the model and that may convey some water through the marsh. A value of Manning's n of 0.04 was assigned to most canal bottoms. However, one row of elements upstream and one row of elements downstream from each canal plug were assigned a Manning's n value of 0.10. The partially filled subreach of canal reach BH between the sixth and seventh plugs from the north also was assigned a Manning's value of 0.10. This value of n resulted in a velocity magnitude of 0.25 ft/s at the fifth plug from the north end of canal reach BH. The computed depth at the plug was 1.8 ft. This is in close agreement with the mean, 0.24 ft/s, of the three velocity values of the profile measured at this location on March 22, 1996. Lines of constant water-surface elevation for the calibration simulation are shown in figure 23.

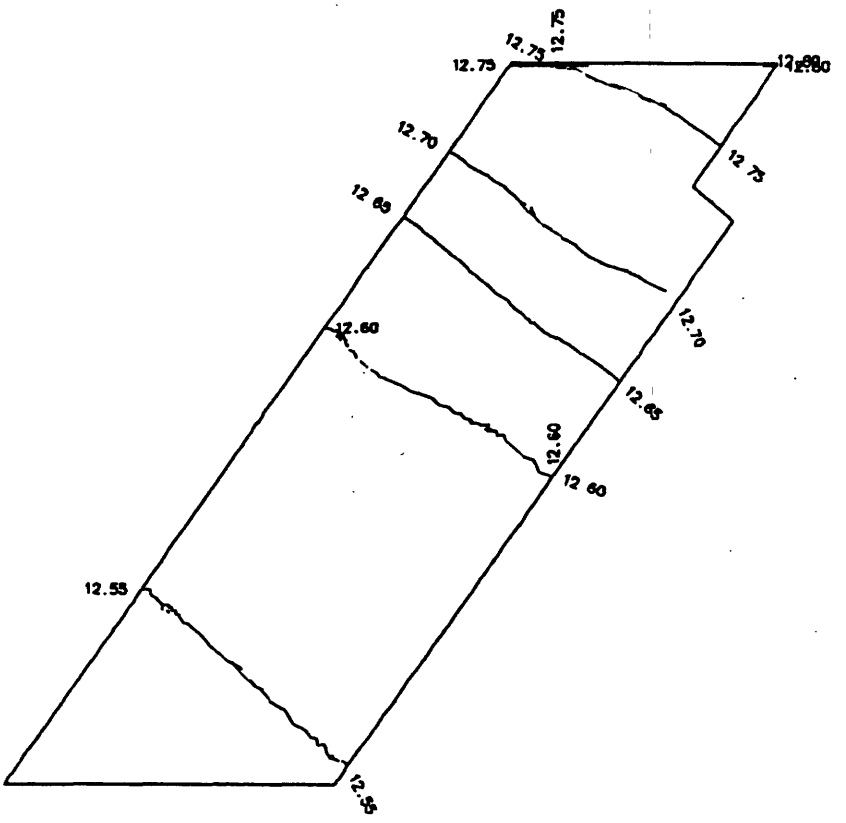

Figure 23: Lines of constant water-surface elevation for the model of Cell 1 of the Everglades Nutrient Removal Project, calibrated with March 17–21, 1996, data. Canals, canal plugs, and wind are represented in the simulation.

Table 4. Observed and computed Cell 1 water-surface elevations.

Station number	Observed water-surface elevation, in feet above sea level	Run C computed water-surface elevation, in feet above sea level	Run NP computed water-surface elevation, in feet above sea level	Run NC computed water-surface elevation, in feet above sea level	Run NW computed water-surface elevation, in feet above sea level
G-252AB$_T$	12.72	12.75	12.74	12.78	12.72
G-252EF$_T$	12.78	12.77	12.76	12.90	12.75
G-252IJ$_T$	12.80	12.78	12.78	13.84	12.76
G-253AB$_H$	12.50	12.52	12.52	12.52	12.52
G-253EF$_H$	12.54	12.53	12.53	12.54	12.53
G-253IJ$_H$	12.55	12.54	12.54	12.55	12.54
ENR101	12.60	12.60	12.60	12.57	12.57

After calibration was completed, computed values of velocity magnitude and direction at and downstream from station ENR101 were compared with the values obtained from the dye release. The computed velocity magnitude and direction are about 0.036 ft/s and 201 degrees, respectively, in the area between station ENR101, the dye-release point, and the locations of the westernmost autosamplers. In addition, in the calibrated model, water flows west in canal reach GH at about 0.12 ft/s. Thus, it seems likely that a combination of marsh flow and canal flow carried the center of mass of the dye cloud west of the autosampler transects on April 4-5, 1996. Nevertheless, the computed velocity magnitude 0.036 ft/s is in reasonable agreement with the velocity magnitudes obtained from the dye release, 0.039 and 0.021 ft/s.

Plots of computed canal discharge as a function of distance along the canal reach are shown in figures 24 through 29 for canal reaches AC, BH, FI, EM, JK, and LM, respectively. These plots will be discussed in more detail after three additional simulations are presented in the next section.

Determining Effects of Canals, Canal Plugs, and Wind

Three additional simulations were performed in which various features of the calibrated model were changed:

- Simulation of Cell 1 without plugs in the canals and with all other features the same as in the calibrated model;
- Simulation of Cell 1 without wind and with all other features the same as in the calibrated model; and
- Simulation of Cell 1 without canals and with all other features the same as in the calibrated model.

In simulating the removal of the canal plugs, the ground-surface elevation at each of the 14 nodes at which plugs were present in the calibrated model was set to the ground-surface elevation of the adjacent canal bottom. The value of Manning's n for the rows of elements immediately upstream and downstream from the plugs was set to 0.04, the value used for the canal bottoms. The partially filled subreach of canal BH was unchanged. All other features were the same as in the calibrated model. Lines of constant

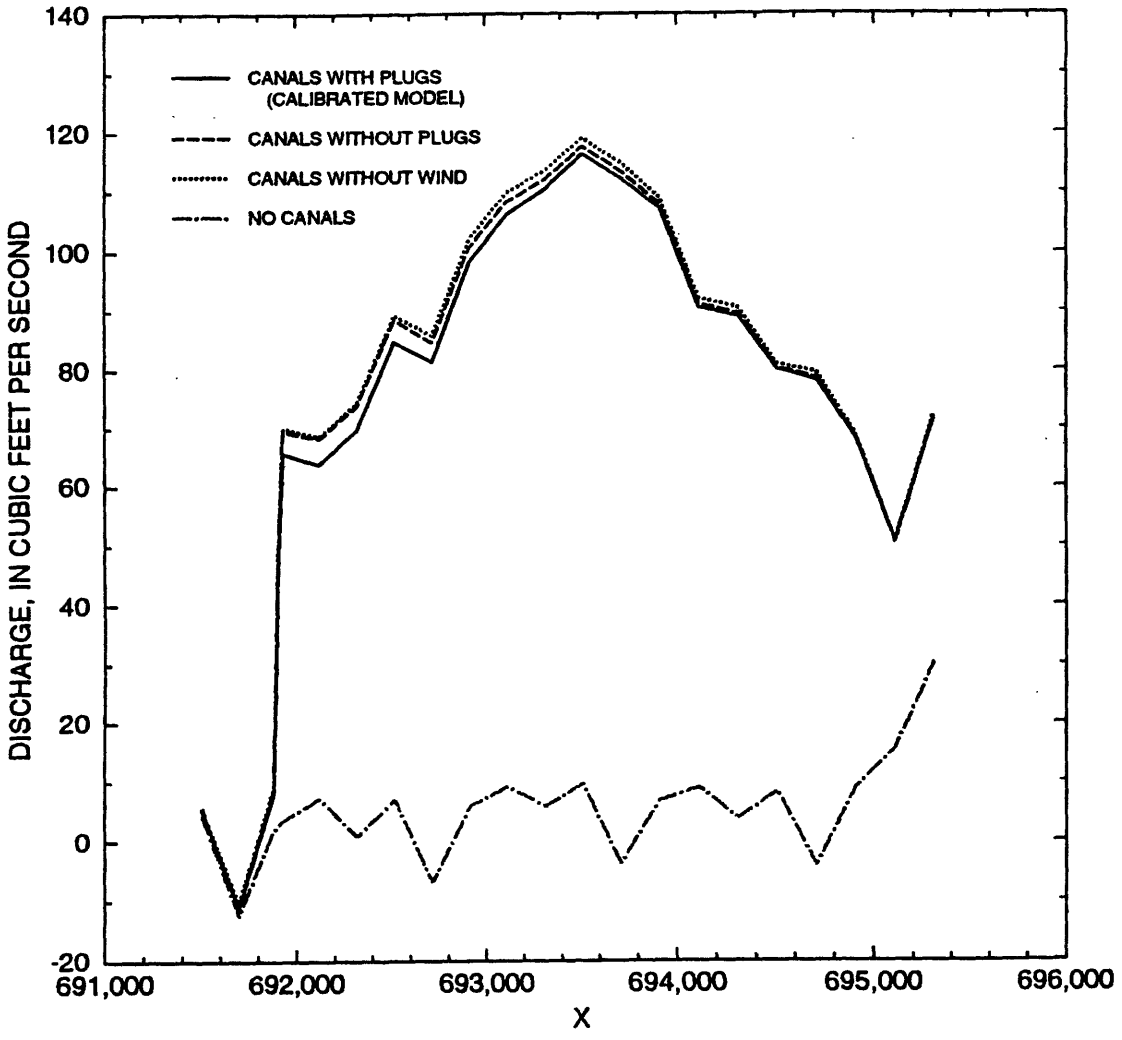

Figure 24: Computed discharge in canal reach AC for canals with plugs, canals without plugs, canals without wind, and no canals, Cell 1, Everglades Nutrient Removal Project, March 17–21, 1996.

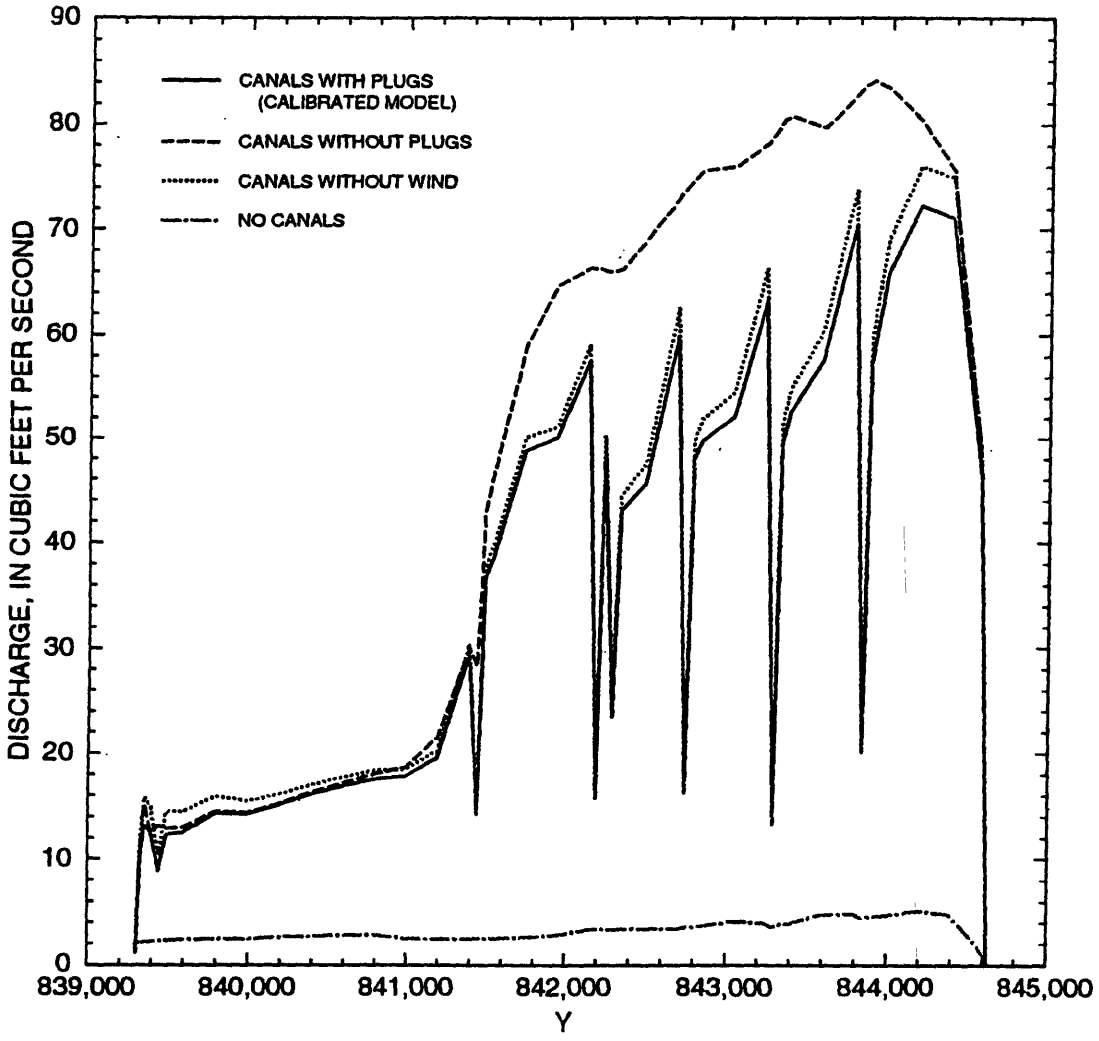

Figure 25: Computed discharge in canal reach BH for canals with plugs, canals without plugs, canals without wind, and no canals, Cell 1, Everglades Nutrient Removal Project, March 17–21, 1996.

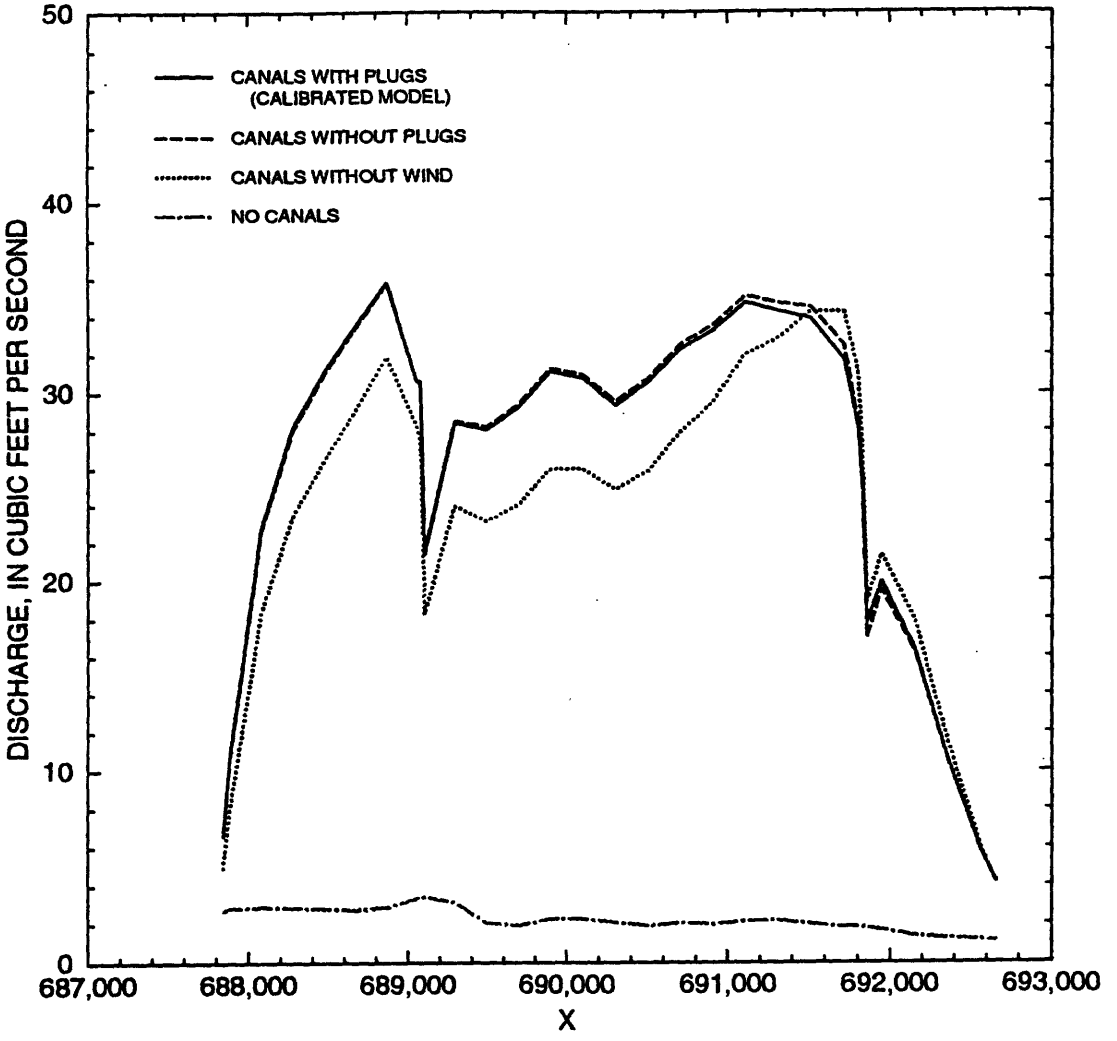

Figure 26: Computed discharge in canal reach FI for canals with plugs, canals without plugs, canals without wind, and no canals, Cell 1, Everglades Nutrient Removal Project, March 17–21, 1996.

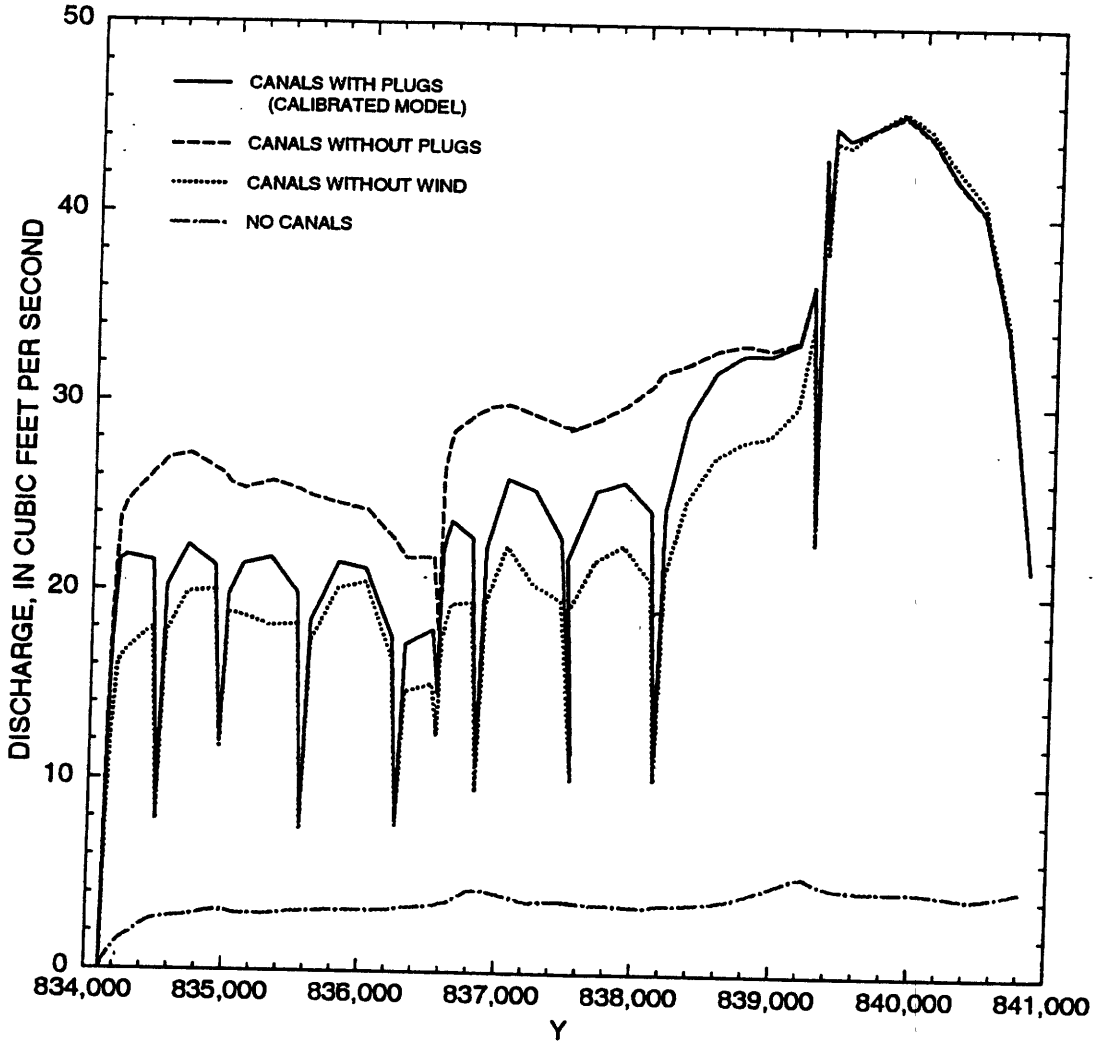

Figure 27: Computed discharge in canal reach EM for canals with plugs, canals without plugs, canals without wind, and no canals, Cell 1, Everglades Nutrient Removal Project, March 17–21, 1996.

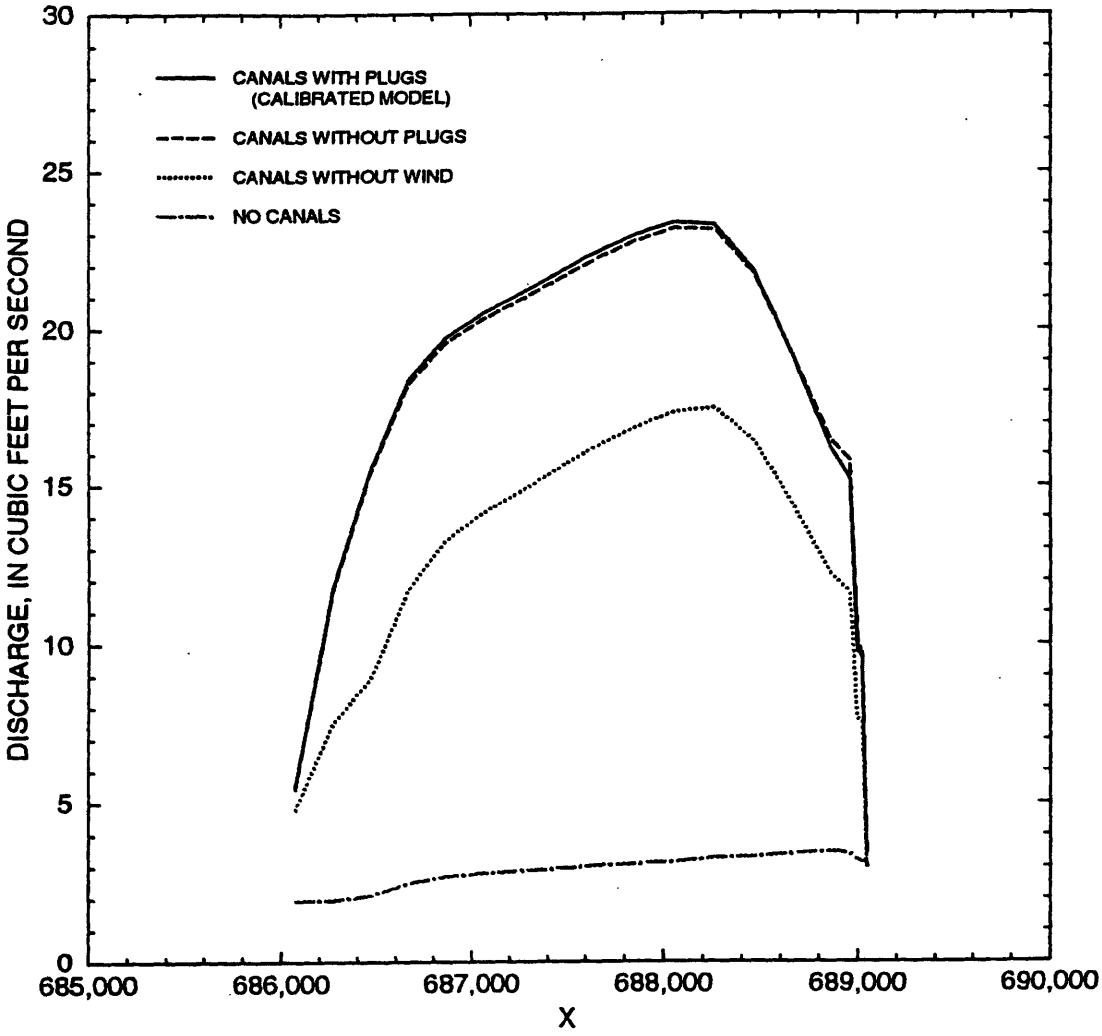

Figure 28: Computed discharge in canal reach JK for canals with plugs, canals without plugs, canals without wind, and no canals, Cell 1, Everglades Nutrient Removal Project, March 17–21, 1996.

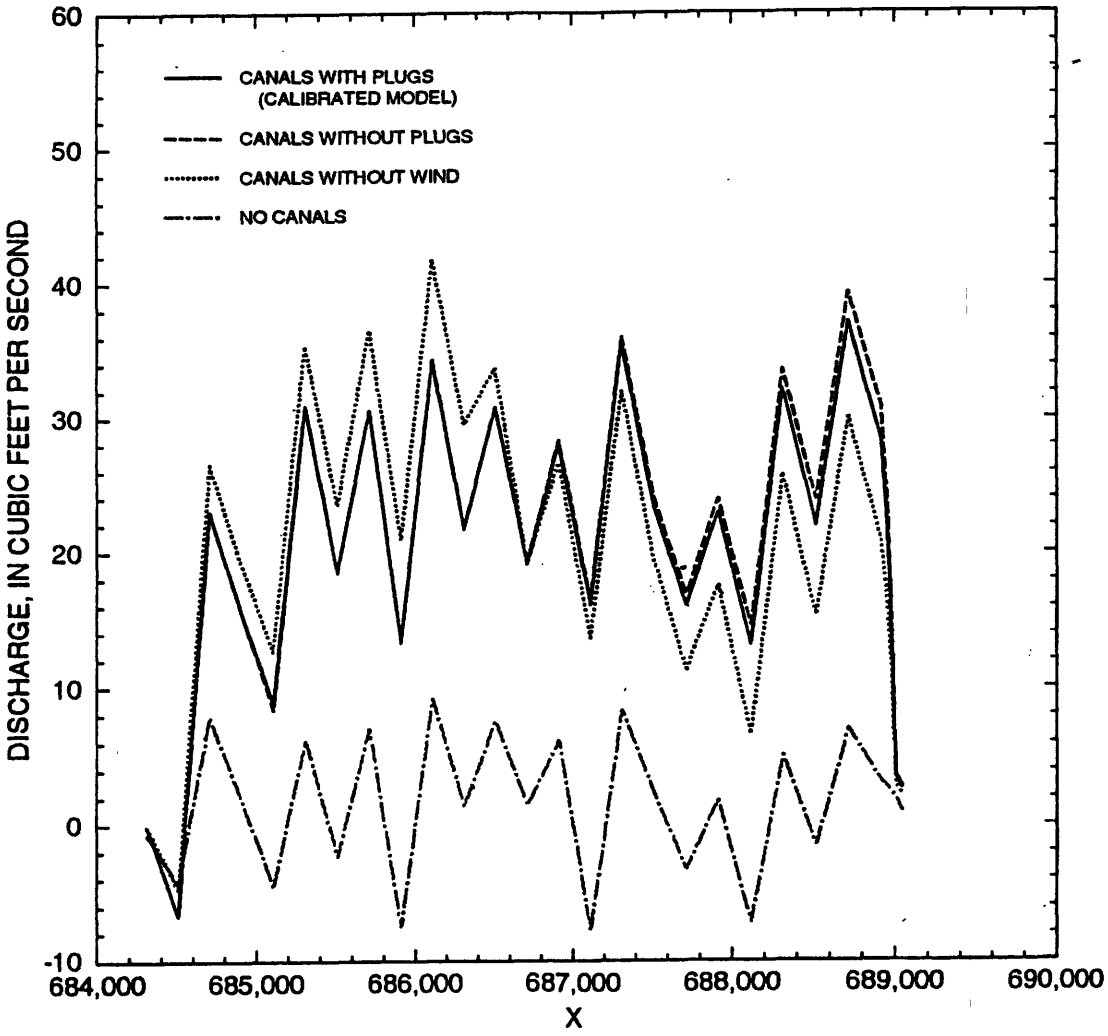

Figure 29: Computed discharge in canal reach LM for canals with plugs, canals without plugs, canals without wind, and no canals, Cell 1, Everglades Nutrient Removal Project, March 17–21, 1996.

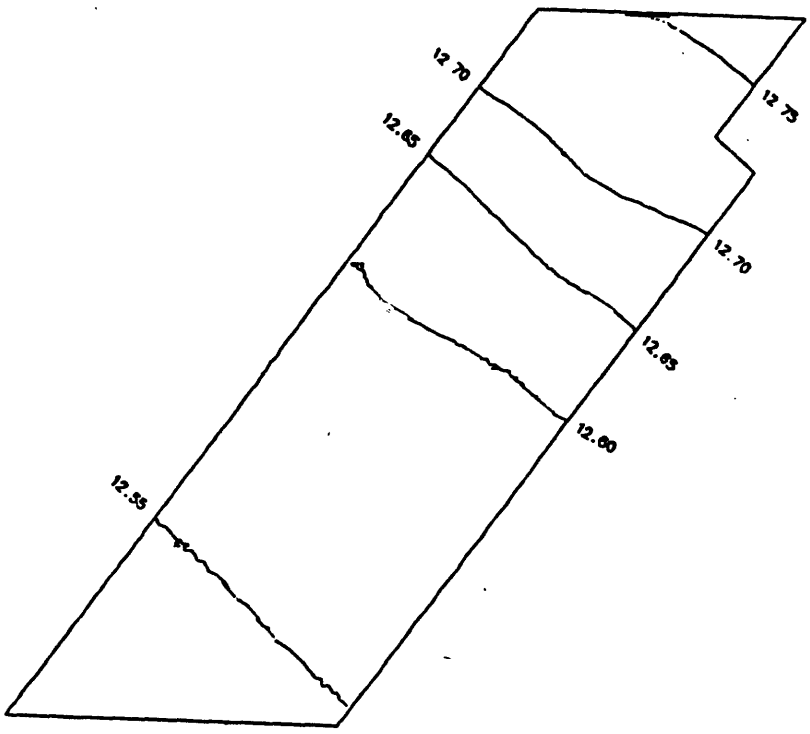

Figure 30: Lines of constant water-surface elevation for the model of Cell 1 of the Everglades Nutrient Removal Project without canal plugs for March 17–21, 1996, data.

water-surface elevation for this simulation are shown in figure 30. Computed water-surface elevations for this simulation are given in the column labeled "Run NP" of table 4.

To simulate no wind, the wind code in the input data for the calibrated model was changed to zero. All other features were the same as in the calibrated model. Lines of constant water-surface elevation for this simulation are shown in figure 31, and computed water-surface elevations are given in the column labeled "Run NW" of table 4.

To simulate a system without canals, the (TRIGRID) grid generated before canal-bottom and berm elevations were added was used as the basis for the simulation. Thus, the topography of this system is represented in figure 20. The value of Manning's n for elements that were formerly canal bottoms was set to the value (0.18) for shallow open water with submersed vegetation or the value (0.27) for cattail marsh, as appropriate. Lines of constant water-surface elevation for this simulation are shown in figure 32, and computed water-surface elevations are given in the column labeled "Run NC" of table 4.

In general, the results indicate that flow in Cell 1 is in a south-southwest direction, parallel to the levees forming the east and west boundaries of the cell. As a consequence of this, water flows from north to south in the canals aligned in a north-south direction and from east to west in the canals aligned in a east-west direction. Canal discharge is affected by canal size and location, the presence of plugs, wind, and culvert inflows and outflows.

Canal AC carries a large amount of flow from east to west adjacent to the north boundary of the Cell 1 (fig. 24). The discharge is greatest near the middle of the reach. Model results show that when this canal is removed, the water-surface drop from station G-252IJ$_T$ to station G-252AB$_T$ increases from 0.03 ft to 1.06 ft (table 4).

The partially filled subreach of canal BH carries much less water than the unfilled subreach when no plugs are present (fig. 25). Plugs reduce the discharge in the unfilled subreach, but the flow between plugs is still substantial.

Wind has an effect in the southern half of Cell 1, where there is much shallow open water with submersed vegetation and the sheltering effect of emergent vegetation is limited to scattered areas of cattails (figs. 26–28). Wind from the southwest (against the direction of water flow in Cell 1) increases flow to the south and west in the canals FI, EM, and JK. Wind retards the shallow, low-inertia open water more than the deep, high-inertia

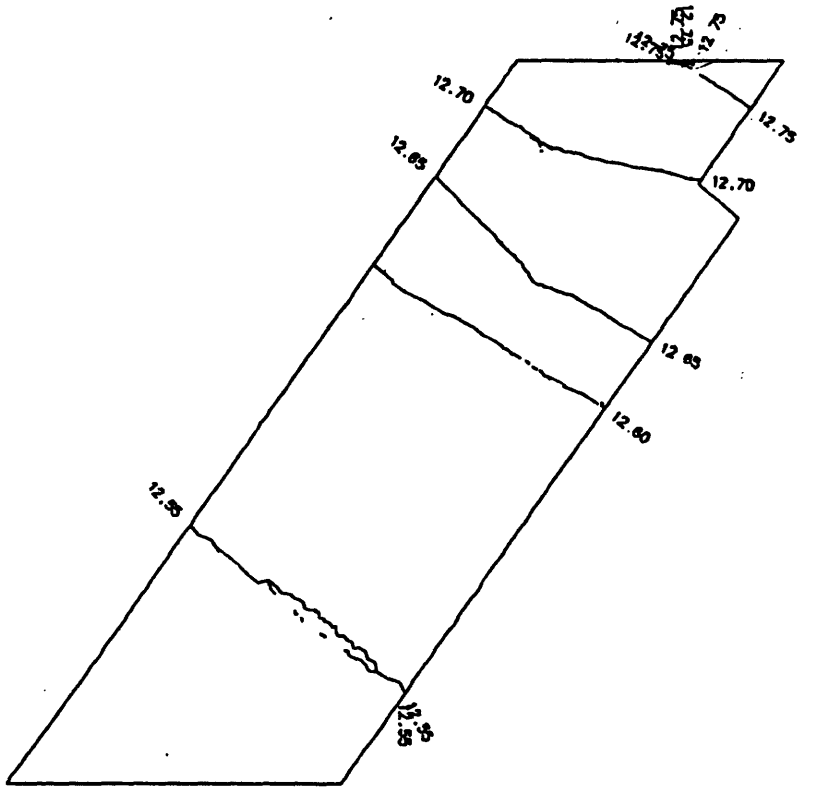

Figure 31: Lines of constant water-surface elevation for the model of Cell 1 of the Everglades Nutrient Removal Project without wind for March 17–21, 1996, data.

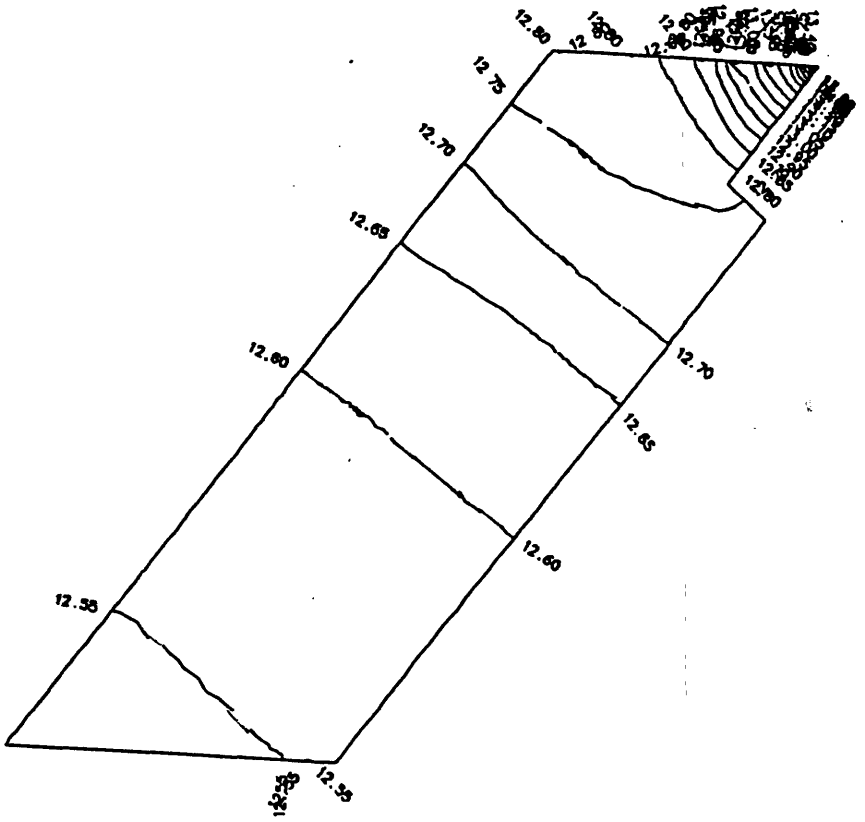

Figure 32: Lines of constant water-surface elevation for the model of Cell 1 of the Everglades Nutrient Project without canals for March 17–21, 1996, data.

canal water. Also, model results indicate that nearly half of the drop in water-surface elevation between stations ENR101 and G-253EF$_H$ is due to the effect of wind (table 4).

Changes in discharge at canal intersections G, H, and K (fig. 21) also are shown in figures 26 and 27. Water flowing south in canal reach EM is partially diverted to the west at both intersections G and K. There is an increase in discharge in canal FI west of intersection G, where some of the water flowing south in subreach EG is diverted to the west into subreach FG.

The effect of the plugs in canal reach EM can be seen in figure 27 by comparing discharge for the runs with and without the plugs in place. When the plugs are present, reductions of about 10 to 20 ft^3/s result at the plugs. The reductions are about 5 ft^3/s or less between plugs.

Large changes in discharge in canal LM are due to the presence of the outflow culverts (fig. 29). The overall direction of flow is from east to west. The effect of wind also is seen in this figure. The southwest wind increases flow in the canal EM and decreases flow in the shallow open areas. Thus, wind causes greater flows in the eastern half of canal LM, which is fed by canal EM, and smaller flows in the western half, where marsh flows from the north are reduced.

Mean hydraulic residence time, defined as the mean volume of water in a water body divided by the mean inflow, is a useful concept, which often can be related to nutrient-removal efficiency. To obtain the mean hydraulic residence time for each of the four simulations of Cell 1, the flow model was used to compute the water volume for each flow solution by integrating the depth, H, over each element and summing over all elements. The water volume is 1.07×10^8 ft^3 for the calibration simulation and the simulation with the plugs removed, 1.06×10^8 ft^3 for the simulation without wind, and 1.04×10^8 ft^3 for the simulation without canals. The model area is 4.86×10^7 ft^2; consequently, the mean depth is 2.20 ft for the calibration simulation and the simulation without plugs, 2.18 ft for simulation without wind, and 2.14 ft for the simulation without canals. Because the mean total inflow is 351.7 ft^3/s in all cases, the mean hydraulic residence time is 3.52, 3.52, 3.49, and 3.42 d for the simulation with canals and plugs, with canals and without plugs, with canals and without wind, and with wind and without canals, respectively. Thus, the mean hydraulic residence time provides little information about the effect of canals on the movement of water through Cell 1. Useful information could be obtained from the distribution of residence times of different parcels of water introduced in the inflow into Cell 1 with a

particle-tracking model.

Summary and Conclusions

A model for surface-water flow in wetlands was developed by adding new features to a two-dimensional, depth-averaged finite-element model for surface-water flow, FESWMS-2DH. The enhanced model accounts for precipitation, evapotranspiration, ground-water inflow/outflow, levee seepage, the sheltering of the water surface from wind by emergent vegetation, and the effects on culvert flow, weir-segment flow, and levee-segment seepage of water-surface elevations outside the wetland. These model enhancements are described in Lee (1997).

The model was implemented for Flow-Way Cell 1 of the Everglades Nutrient Removal Project with data collected during the period March 17–21, 1996. Inflows, outflows, and water-surface elevations in Cell 1 changed little during this period. A persistent southwest wind was recorded during the 5-day period. The grid-generation software TRIGRID was used to develop a finite-element grid for Cell 1 that represented the topography and vegetation of the cell. Seven earthen plugs in each of two north-south canals were represented in the grid. Model calibration required the adjustment of flow-resistance coefficients, culvert discharge coefficients, hydraulic conductance, and levee permeabilities to obtain agreement between observed and computed water-surface elevations, flow velocities, culvert discharges, and levee seepage. Additional simulations were performed for canals without plugs, canals with plugs but without wind, and no canals.

The following results were obtained from the simulations:

- Manning's n values of 0.27 for cattail marsh with numerous small ditches and 0.18 for shallow open water with submersed vegetation and sugar-cane stubble gave close agreement between observed and computed water-surface elevations and velocities.

- Water on marsh with either submersed or emergent vegetation flowed toward the south southwest, parallel to the levees on the east and west sides of Flow-Way Cell 1.

- Water flowed from north to south in north-south canals and from east to west in east-west canals.

- Canal plugs caused a large reduction in canal discharge at the plugs and a small reduction in canal discharge between plugs.
- Wind had an appreciable effect on flow distribution and water-surface slope in the southern half of Cell 1, where much of the marsh was open with submersed vegetation.

References

Abtew, W., 1996, Evapotranspiration measurements and modeling for three wetland systems in south Florida: Water Resources Bulletin, v. 32, no. 3, p. 465-473. Abtew, W., and Khanal, N., 1994, Water budget analysis for the Everglades

Agricultural drainage basin: Water Resources Bulletin, v. 30, no. 3, p. 429–439.

Bodhaine, G. L., 1968, Measurement of peak discharge at culverts by indirect methods: U.S. Geological Survey Techniques of Water-Resources Investigations, book 3, chap. A3, 68 p.

Department of the Army, Office of the Chief of Engineers, 1978, Design and construction of levees: Washington, D.C., Department of the Army, Office of the Chief of Engineers, Engineer Manual 1110-2-1913.

Froehlich, D. C., 1989, Finite element surface-water modeling system: Two-dimensional flow in a horizontal plane. Vol. I. Users manual: McLean, Va., U.S. Department of Transportation, Federal Highway Administration, Publication No. FHWA-RD-88-177, 286 p.

Guardo, Mariano, 1996, Hydrologic balance for a subtropical treatment wetland constructed for nutrient removal, *in* xxxx, ed., xxxxx: Annual Conference and Symposium on GIS and Water Resources, 32nd, Ft. Lauderdale, Fla., 1996, Proceedings: American Water Resources Association, p. xx–xx.

Guardo, Mariano, Abtew, W., Obeysekera, J., and Roy, J., 1994, The Everglades Nutrient Removal Project: Hydrology, hydrodynamics and operation, *in* Palombo, A. J., and others, eds.: Interamerican Dialogue on Water Management, 1st, Miami, Fla., 1993, Proceedings: Miami, Fla., xxx, p. 171–181.

Guardo, Mariano, Fink, L., Fontaine, T. D., Newman, S., Chimney, M. J., Bearzotti, R., and Goforth, G., 1995, Large-scale constructed wetlands

for nutrient removal from stormwater runoff: An Everglades restoration project: Environmental Management, v. 19, no. 6, p. 879–889.

Jammal and Associates, Inc., 1991, Geotechnical services, SFWMD Everglades Nutrient Removal Project: West Palm Beach, Fla., Jammal and Associates, Inc., 17 p.

Lee, J. K., 1998, Finite-element surface-water modeling system: Two-dimensional flow in the horizontal plane—Addendum to the users manual: U.S. Geological Survey Open-File Report 97-410, 74 p.

Lee, J. K., and Froehlich, D. C., 1989, Two-dimensional finite-element hydraulic modeling of bridge crossings: Research report: McLean, Va., U.S. Department of Transportation, Federal Highway Administration, Publication No. FHWA-RD-88-146, 290 p.

Lynch, D. R., 1986, Basic hydrodynamic equations for lakes, *in* Gray, W. G., ed., Physics-based modeling of lakes, reservoirs, and impoundments: New York, American Society of Civil Engineers, p. 17–53.

McDonald, M. G., and Harbaugh, A. W., 1988, A modular three-dimensional finite-difference ground-water flow model: U.S. Geological Survey, Techniques of Water-Resources Investigations, book 6, chap. A1, 586 p.

Peter, Pavel, 1982, Canal and river levees: New York, Elsevier, 540 p.

Pinder, G. F., and Gray, W. G., 1977, Finite element simulation in surface and subsurface hydrology: New York, Academic Press, 295 p.

Prymas, A. A., 1997, Calibration of seepage from steady state simulations for water budget estimation: Boca Raton, Fla., Florida Atlantic Univeristy, Department of Ocean and Civil Engineering, unpublished thesis, 76 p.

Reid, R. O., and Whitaker, R. E., 1976, Wind-driven flow of water influenced by a canopy: Proceedings of the American Society of Civil Engineers, v. 102, no. WW1, p. 61–77.

South Florida Water Management District, 1994, Vegetation map of the Everglades Nutrient Removal Site with gauge locations, October 14, 1994: West Palm Beach, Fla., South Florida Water Management District, Department of Ecosystem Research and Implementation, Everglades Systems Research Division, Natural Systems Unit, and Department of Water Resource Evaluation, Hydrologic Data Management Division, 1 sheet.

Walters, R. A., and Henry, R. F., 1997, TRIGRID users manual (GKS version): 150 p.

Zienkiewicz, O. C., 1977, The finite element method (3d ed.): London, Mc-

Graw-Hill, 787 p.

Lee and Guardo – A Finite-Element Surface-Water Model of Cell 1 of the Everglades Nutrient Removal Project
U.S. Geological Survey Water-Resources Investigations Report 97-4159